Organometallics **1989**, *8*, 119-132

6-Methyl-2,4,7-nonatriene: ^{1}H NMR (CDCl$_3$) δ 5.35–5.65 (m, 6 H, CH=), 2.69 (m, 1 H, CH$_3$ at C(6)), 1.65 (b s, CH$_3$ at C(1) and C(9)), 0.99 (d, 3 H, J = 7.6 Hz, CH$_3$ at C(6)); EIMS, m/z 136 (M$^+$).

4-Methyl-1,3,6-nonatriene: ^{1}H NMR (CDCl$_3$) δ 6.68 (dt, 1 H, J = 16.1 and 10.8 Hz, CH= at C(2)), 6.05 (m, 2 H, CH= at C(6) and C(7)), 5.40 (m, 1 H, CH= at C(3)), 5.15 (m, 2 H, CH$_2$=), 2.18 (d, 2 H, J = 6.2 Hz, CH$_2$), 2.12 (dq, 2 H, J = 7.8 and 6.1 Hz, CH$_2$ at C(8)), 1.64 (s, 3 H, CH$_3$), 0.94 (t, 3 H, CH$_3$); EIMS, m/z 136 (M$^+$).

EPR Measurement. (C$_5$R$_5$)TiCl$_3$ (R = H, Me; 0.1 mmol) dissolved in benzene (10 mL) was reduced with (2-methyl-2-butene-1,4-diyl)magnesium (0.15 mmol) at 25 °C. The solution thus obtained was transferred into an EPR tube (5 mm i.d.) via a syringe in argon, and the tube was sealed. EPR measurements were carried out on a JEOL FE-1X spectrometer with 100-kHz field modulation in conjunction with a cylindrical TE$_{011}$ cavity in the temperature range of 4–320 K. The g value was obtained in a conventional method by using Mn^{2+} in MgO as a standard.

Acknowledgment. We are indebted to Grant-in-Aid for Special Project Reseach (No. 61225015 and No. 62115007) from the Ministry of Education, Science and Culture, Japan. We also thank Prof. M. Kamachi of Osaka University for the measurement of EPR spectra.

Registry No. **1a**, 114802-64-1; **1b**, 117559-23-6; **1c**, 117559-24-7; **2a**, 114802-65-2; **2b**, 117559-25-8; **3a**, 114802-63-0; **3b**, 117559-26-9; **4**, 106457-12-9; **5**, 117559-27-0; **6a**, 117559-28-1; **6b**, 117559-29-2; **8**, 117559-30-5; **9**, 117559-31-6; C$_5$Me$_5$SiMe$_3$, 87778-95-8; (C$_5$Me$_5$)TiCl$_3$, 12129-06-5; (C$_5$Me$_5$)TiBr$_3$, 33151-84-7; (C$_5$Me$_5$)TiI$_3$, 102261-45-0; (C$_5$Me$_5$)$_2$TiCl$_2$, 11136-36-0; pentamethylcyclopentadiene, 4045-44-7; (2-butene-1,4-diyl)magnesium, 70809-00-6; (1,4-diphenyl-2-butene-1,4-diyl)magnesium, 114872-27-4; (2-methyl-2-butene-1,4-diyl)magnesium, 90823-62-4; (2,3-dimethyl-2-butene-1,4-diyl)magnesium, 95251-09-5; (2,3-diphenyl-2-butene-1,4-diyl)magnesium, 117527-70-5; 1,3-butadiene, 106-99-0; 1,4-diphenyl-1,3-butadiene, 886-65-7; 2-methyl-1,3-butadiene, 78-79-5; 2,3-diphenyl-1,3-butadiene, 2548-47-2; isoprene, 78-79-5; 2,3-dimethyl-1,3-butadiene, 513-81-5; (E)-1,3-pentadiene, 2004-70-8; 2,6-dimethyl-1,3,6-octatriene, 2431-45-0; 3,6-dimethyl-1,3,6-octatriene, 32778-25-9; 2,6-dimethyl-2,4,6-octatriene, 673-84-7; 2,3,6,7-tetramethyl-1,3,6-octatriene, 117527-68-1; 6-methyl-2,4,7-nonatriene, 36718-48-6; 4-methyl-1,3,6-nonatriene, 117527-69-2; 1,3-pentadiene, 504-60-9.

Supplementary Material Available: Listing of final atomic coordinates for hydrogen atoms with thermal parameters and bond distances and angles including hydrogen atoms (11 pages); listings of calculated structure factors (85 pages). Ordering information is given on any current masthead page.

Chemistry of (μ-Dithio)bis(tricarbonyliron), an Inorganic Mimic of Organic Disulfides. 3. Reaction with Low-Valent Metal Compounds and Some Interesting Isolobal Analogies Involving the Products[1]

Martin Cowie*

Department of Chemistry, University of Alberta, Edmonton, Alberta, Canada T6G 2G2

Roger L. DeKock* and Timothy R. Wagenmaker

Department of Chemistry, Calvin College, Grand Rapids, Michigan 49506

Dietmar Seyferth,* Richard S. Henderson, and Michael K. Gallagher

Department of Chemistry, Massachusetts Institute of Technology, Cambridge, Massachusetts 02139

Received March 7, 1988

The analogy between (μ-S$_2$)Fe$_2$(CO)$_6$ and organic disulfides extends to reactions with low-valent metal species. The following zerovalent metal phosphine complexes and (organo)metal carbonyls react with (μ-S$_2$)Fe$_2$(CO)$_6$: (Ph$_3$P)$_4$Pt, (Ph$_3$P)$_3$PdCO, (diphos)Ni(CO)$_2$, (η^5-C$_5$H$_5$)$_2$Ti(CO)$_2$, (η^5-C$_5$H$_5$)Co(CO)$_2$, (η^5-C$_5$Me$_5$)Co(CO)$_2$, [(η^5-C$_5$H$_5$)Co(μ-CO)]$_2$, Co$_2$(CO)$_8$, Fe$_2$(CO)$_9$, Fe(CO)$_2$(NO)$_2$. In all cases, initial attack appears to occur at the S–S bond of (μ-S$_2$)Fe$_2$(CO)$_6$. Two products of these reactions, (η^5-C$_5$Me$_5$)Co(μ_3-S)$_2$Fe$_2$(CO)$_6$ and [(η^5-C$_5$Me$_5$)Co(μ-CO)]$_2$(μ_3-S)$_2$Fe$_2$(CO)$_6$, have been structurally characterized by X-ray crystallography. The former crystallizes in the orthorhombic space group $P2_12_12_1$ with a = 8.848 (5) Å, b = 12.571 (3) Å, c = 18.707 (3) Å, and Z = 4. Refinement has converged at R = 0.058 and R_w = 0.051 based on 2031 unique observations (NO) and 244 parameters varied (NV). This heteronuclear cluster has a structure in which the Co atom is sandwiched between the C$_5$Me$_5$ group and the four-membered, heteroatom ring of the (μ-S)$_2$Fe$_2$(CO)$_6$ moiety, which in the observed geometry, is isolobal with cyclobutadiene. Cobalt is bonded to the Fe and S atoms, but there is no Fe–Fe bond. A rationalization for the observed structure, based on Fenske–Hall Calculations, is presented. The structural parameters for the second species are as follows: monoclinic space group $P2_1/m$, a = 10.712 (1) Å, b = 14.837 (2) Å, c = 10.8215 (9) Å, β = 115.537 (8)°, Z = 2, R = 0.033, R_w = 0.040, NO = 2409, and NV = 202. This structure has resulted from the apparent insertion of the (η^5-C$_5$Me$_5$)$_2$Co$_2$(μ-CO)$_2$ moiety into the S–S bond of the Fe$_2$(μ_2-S$_2$)(CO)$_6$ "butterfly", such that the two fragments are linked by two Co–S bonds. The Co–Co bond lies essentially parallel to the S–S axis and perpendicular to the Fe–Fe bond.

Introduction

Some reactions of (μ-dithio)bis(tricarbonyliron) (1) which we have reported previously are ones typical of diorgano disulfide reactivity: reduction of the S–S bond by sodium metal and by metal hydrides[1b] and nucleophilic cleavage by organolithium and Grignard reagents.[1a] We were interested in determining whether this analogy between the S–S bond reactivity of (μ-S$_2$)Fe$_2$(CO)$_6$ and RSSR extended to insertion reactions of coordinatively unsaturated, low-valent transition-metal species into the re-

---

[1] (a) Part 2: Seyferth, D.; Henderson, R. S.; Song, L.-C.; Womack, G. B. *J. Organomet. Chem.* **1985**, *292*, 9. (b) Seyferth, D.; Henderson, R. S.; Song, L.-C. *Organometallics* **1982**, *1*, 125.

0276-7333/89/2308-0119$01.50/0

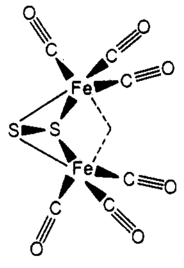

1

spective S–S bonds and to more complicated reactions with metal carbonyls.

Coordinatively unsaturated, low-valent metal species have been shown to insert into the S–S bond of both acyclic[2] and cyclic[3] organic disulfides (eq 1). Some examples are those shown in eq 2–4. However, at the time that this work was initiated, little was known about the reactivity of related *inorganic* disulfides such as $(\mu\text{-}S_2)Fe_2(CO)_6$ (1). In one previous study Markó and co-workers[4] described the reaction of 1 with $Co_2(CO)_8$ in hexane at room temperature giving 2 in 56% yield. (In our hands, this reaction (20 h at room temperature in THF) produced 2 in 98% yield). This product is not as expected for simple insertion into the S–S bond of 1 and suggests that analogies between 1 and organic disulfides may not extend to reactions with low-valent transition metal complexes.

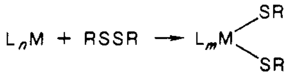

$$L_nM + RSSR \rightarrow L_mM\begin{matrix}SR\\SR\end{matrix} \qquad (1)$$

$m = n$ or $m < n$ when a ligand is released from L_nM

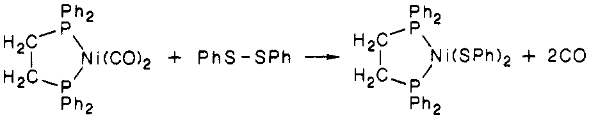

(2)

$$(Ph_3P)_4M + PhS{-}SPh \rightarrow (Ph_3P)_2M(SPh)_2 + 2PPh_3 \qquad (3)$$

M = Pd, Pt

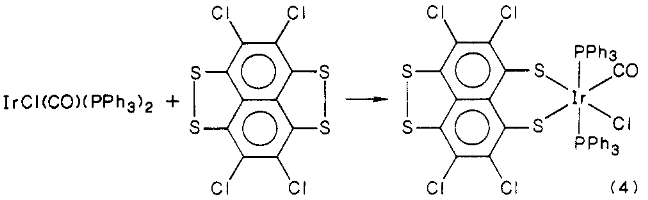

(4)

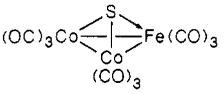

2

Theoretical studies[5] of $(\mu\text{-}S_2)Fe_2(CO)_6$ indicate that the HOMO consists of an Fe–Fe bond, best described as a "bent" single bond, and the LUMO consists of S–S π^* character.[5b] While these calculations are capable of explaining why the S–S bond is ruptured rather than the Fe–Fe bond in a two-electron reduction to form the dianion,[6] it is not clear that one would predict such exclusive reactivity at the S–S bond regardless of whether the reactant is electrophilic or nucleophilic. (The crystallographic work on $(\mu\text{-}S_2)Fe_2(CO)_6$ shows that the S–S bond is a "normal" single bond with an S–S distance of 2.007 (5) Å.[7])

In the absence of mechanistic information of any of these reactions, an empirical bond energy argument provides the best rationalization for the cleavage of the S–S bond. Consider the following hypothetical reaction[8] by way of example. In case A an S–S (single) bond is broken and two Ge–S bonds are formed. In case B we have broken an Fe–Fe bond and formed two Fe–Ge bonds. Using diatomic bond strengths as a guide,[9] we predict a release of 161.75 kcal/mol for case A and 76.8 kcal/mol for case B. Clearly, the diatomic bond strengths are not ideal guidelines since both the S_2 and GeS diatomic molecules contain multiple bonds; single bond strengths might well reduce each of the quoted numbers for S_2 and GeS by 30 kcal/mol (the Cl_2 single bond has a strength[9] of 58 kcal/mol). Even with this reduction, and assuming no corresponding reduction for the Fe–Ge and Fe–Fe values, case A results in a release of about 100 kcal/mol compared to about 75 kcal/mol for case B. We feel that this energetic reason alone is sufficient to account for the observed reactivity of the S–S bond. These arguments, as applied to the reactant "$GeCl_2$", can also be applied to a number of other reactants such as $LiCH_3$ and L_2M (M = Ni, Pd, and Pt).

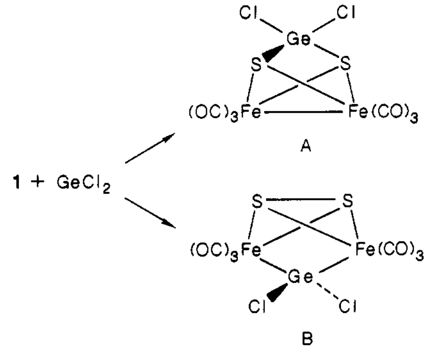

In this paper we report an investigation of the reactions of several low-valent metal complexes with $(\mu\text{-}S)_2Fe_2(CO)_6$ and the X-ray structure determinations of two of the products. Although the structure of one product, $[(\eta^5\text{-}C_5Me_5)Co(\mu\text{-}CO)]_2(\mu\text{-}S)_2Fe_2(CO)_6$, is consistent with the predicted reactivity at the S–S bond of the precursor, the

---

[2] (a) King, R. B.; Treichel, P. M.; Stone, F. G. A. *J. Am. Chem. Soc.* **1961**, *83*, 3600. (b) King, R. B.; Bisnette, M. B. *Inorg. Chem.* **1965**, *4*, 482. (c) Hayter, R. G.; Humiec, F. S. *J. Inorg. Nucl. Chem.* **1964**, *26*, 807. (d) Zanella, R.; Ros, R.; Graziana, M. *Inorg. Chem.* **1974**, *12*, 2737. (e) Lam, C. T.; Senoff, C. V. *Can. J. Chem.* **1972**, *50*, 1868. (f) Markham, Y. L.; Chung, G. D.; Branum, G. D.; Blake, D. M. *J. Organomet. Chem.* **1976**, *107*, 121. (g) de Croon, M. H. J. M.; van Gaal, H. L. M.; van der Ent, A. *Inorg. Nucl. Chem. Lett.* **1974**, *10*, 1081. (h) Fachinetti, G.; Floriani, C. *J. Chem. Soc., Dalton Trans.* **1974**, 2433. (i) Werner, J.; Juthani, B. *Z. Anorg. Allg. Chem.* **1981**, *473*, 107.

[3] (a) King, R. B. *Inorg. Chem.* **1963**, *2*, 641. (b) Davison, A.; Edelstein, N.; Holm, R. H.; Maki, A. H. *Inorg. Chem.* **1963**, *2*, 817. (c) Teo, B. K.; Wudl, F.; Marshall, J. H.; Kruger, A. *J. Am. Chem. Soc.* **1977**, *99*, 2349. (d) Gal, A. W.; Gosselink, J. W.; Vollenbroek, F. A. *Inorg. Chem. Acta* **1979**, *32*, 235. (e) Teo, B. K.; Snyder-Robinson, P. A. *Inorg. Chem.* **1978**, *17*, 3489. (f) Teo, B. K.; Snyder-Robinson, P. A. *J. Chem. Soc., Chem. Commun.* **1979**, 255. (g) Drozd, V. N.; Sokolov, V. I.; Sergeichuk, V. V. *Izv. Akad. Nauk SSSR, Ser. Khim.* **1981**, 1624. (h) Teo, B. K.; Snyder-Robinson, P. A. *Inorg. Chem.* **1981**, *20*, 4235.

[4] Khattab, S. A.; Markó, L.; Bor, G.; Markó, B. *J. Organomet. Chem.* **1964**, *1*, 373.

[5] (a) Teo, B. K.; Hall, M. B.; Fenske, R. F.; Dahl, L. F. *Inorg. Chem.* **1975**, *14*, 3103. (b) DeKock, R. L.; Baerends, E. J.; Hengelmolen, R. *Organometallics* **1984**, *3*, 288. (c) DeKock, R. L.; Baerends, E. J.; Oskam, A. *Inorg. Chem.* **1983**, *22*, 4158.

[6] Wetherhill, T. D.; Rauchfuss, T. B.; Scott, R. A. *Inorg. Chem.* **1986**, *25*, 1466.

[7] Wei, C. H.; Dahl, L. F. *Inorg. Chem.* **1965**, *4*, 1.

[8] $GeCl_2$ complexes formed from various precursors do exist, see ref 1b and: Nametkin, N. S.; Tyurin, V. D.; Aleksandrov, G. G.; Kuz'min, O. V.; Nekhaev, A. I.; Andrianov, V. G.; Marlonov, M.; Struchkov, Yu. T. *Izv. Akad. Nauk SSSR, Ser. Khim.* **1979**, 1353.

[9] Weast, R. C.; Ed. *CRS Handbook of Chemistry and Physics*, 67th ed.; CRC Press: Boca Raton, FL, 1986; pp F-167 to F-177. The relevant values are as follows: Fe–Fe (24 kcal mol^{-1}), Fe–Ge (50.4 kcal mol^{-1}), S–S (101.65 kcal mol^{-1}), and Ge–S (131.7 kcal mol^{-1}).

structure of (η^5-C_5Me_5)Co(μ-S)$_2$$Fe_2(CO)_6$ indicates that it is formed by a somewhat more complex route. A rationalization for the structure of this latter species is presented. In this rationalization we make no attempt to use the frontier orbital character of the fragments to explain the reactivity of the S–S bond, since that is best understood within the framework of the bond strength arguments given above. Rather, we employ the Fenske–Hall calculational method[10] to explore the evolution of the frontier orbitals of (μ-S_2)$Fe_2(CO)_6$ as a function of the dihedral angle between the two Fe_2S planes. This angle is about 65° in the parent compound; it increases to 95° in a model compound such as $GeCl_2Fe_2S_2(CO)_6$ and to 156.3° in the (η^5-C_5Me_5)Co(μ_3-S)$_2$$Fe_2(CO)_6$ structure reported in this work.

Results and Discussion of Reaction Chemistry

Our present studies on the reactivity of (μ-S_2)$Fe_2(CO)_6$ (**1**) show that attack of low-valent metal species at the S–S bond is a general type of reactivity, much as was the case for organic disulfides. Thus a reaction of $(Ph_3P)_4Pt$ with **1** at room temperature in benzene in the presence of an excess of methyl iodide gave a quantitative yield of the $(Ph_3P)_2Pt$-insertion product **3a**. This species is analogous to the selenium complex $(PPh_3)_2Pt(\mu_3\text{-}Se)_2Fe_2(CO)_6$, the structure of which has been determined.[11] In the absence of CH_3I, the 2 molar equiv of Ph_3P that are released in the reaction from the starting platinum(0) reagent displaced CO from iron and a mixture of products resulted. Methyl iodide, however, reacted more rapidly with the free Ph_3P to form the insoluble phosphonium iodide $[Ph_3PCH_3]I$. As a result, only **3a** was formed. The palladium analogue **3b** also was prepared, starting from $(Ph_3P)_4Pd$, but since this starting compound is insoluble in benzene, its suspension in this solvent was treated with CO at atmospheric pressure to form the soluble $(Ph_3P)_3PdCO$,[12] which on reaction with (μ-S_2)$Fe_2(CO)_6$ in the presence of excess methyl iodide gave **3b** as an air-stable, purple-brown solid. Both **3a** and **3b** were identical with the products of the reactions of the (μ-S_2)$Fe_2(CO)_6$-derived dianion with $(Ph_3P)_2PtCl_2$ and $(Ph_3P)_2PdCl_2$, respectively.[1b] Although the η^2-ethylene complexes $(Ph_3P)_2M(\eta^2\text{-}C_2H_4)$ (M = Pd, Pt) serve equally well in the preparation of **3a** and **3b** from (μ-S_2)$Fe_2(CO)_6$,[13] our procedure appears to be simpler in terms of starting materials used. Similarily the reaction of $[Ph_2PCH_2CH_2PPh_2]Ni(CO)_2$ with (μ-S_2)$Fe_2(CO)_6$ in benzene at room temperature gave the corresponding Ni diphosphine complex **4**, which we assume has the structure shown.

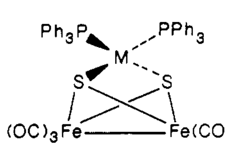

3a, M = Pt
b, M = Pd

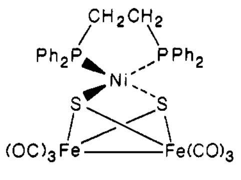

4

The reaction of (η^5-C_5H_5)$Co(CO)_2$ with (μ-S_2)$Fe_2(CO)_6$ in THF at room temperature gave (η^5-C_5H_5)Co(μ-S)$_2$$Fe_2(CO)_6$, as an air-stable black solid, in good yield. This product was identical with that of the (μ-LiS)$_2$$Fe_2(CO)_6$/($\eta^5$-$C_5H_5$)$Co(CO)I_2$ reaction,[1b] which had initially been assigned[1b] structure **5**, in which the Co atom is left electron deficient. In fact a somewhat analogous compound has been characterized, although in this case Co can achieve an 18-electron configuration as shown in **6a** and **6b**.[14] However, the similarity of (η^5-C_5H_5)Co(μ-S)$_2$$Fe_2(CO)_6$ to $Fe_3S_2(CO)_9$[15] has been pointed out by Rauchfuss, who suggested an analogous nido-octahedral structure for the cobalt–iron complex.[16] In order to provide an unambiguous answer to this structural question, we prepared (η^5-C_5Me_5)Co(μ-S)$_2$$Fe_2(CO)_6$ by the reaction of (μ-S_2)$Fe_2(CO)_6$ with (η^5-C_5Me_5)$Co(CO)_2$ and determined its structure by using X-ray crystallography. Although a nido structure is indeed observed for this complex (and presumably the Cp analogue), the isomer obtained is not that expected (**7**) from insertion of the Cp*Co (Cp* = η^5-C_5Me_5) fragment into the S–S bond of (μ-S_2)$Fe_2(CO)_6$, followed by Fe–Co bond formation. Instead structure **8** is obtained, in which insertion of Cp*Co into the S–S bond has been accompanied by flattening of the Fe_2S_2 core, rupture of the Fe–Fe bond, and formation of two Fe–Co bonds. The energetic difference between **7** and **8** is no doubt small, and indeed for the analogous species [(η^5-C_5H_5)$RhTe_2Fe_2(CO)_6$], both isomers corresponding to **7** and **8** have been observed.[17] Nevertheless, there is a simple argument which can be used to predict that **8** would be slightly favored. The difference in bonding between the structures is that **8** has a Fe–Co bond in place of the Fe–Fe bond in **7**. Placing the pair of bonding electrons in the region having the greater nuclear charge (**8**) should stabilize the system. This simple argument is confirmed by an electronegativity perturbation treatment[18a] and indeed was the basis for Pauling's introduction of the concept of electronegativity.[19]

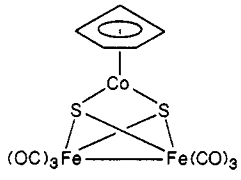

5

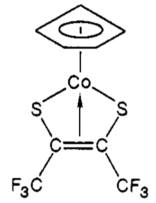

6a

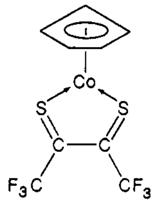

6b

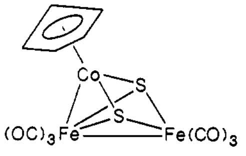

7

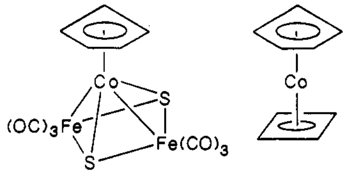

8

Later in the paper we present Fenske–Hall calculations which, along with standard electron counting rules for clusters, make it clear why structure **8** is preferred over structure **5**. We will also show that there is a strong

---

[10] Hall, M. B.; Fenske, R. F. *Inorg. Chem.* **1972**, *11*, 768. Hall, M. B. Ph.D. Thesis, University of Wisconsin, Madison, WI, 1971. Fenske, R. F. *Pure Appl. Chem.* **1971**, *27*, 61.

[11] Day, V. W.; Lesch, D. A.; Rauchfuss, T. B. *J. Am. Chem. Soc.* **1982**, *104*, 1290.

[12] Morandini, F.; Consiglio, G.; Wenzinger, F. *Helv. Chim. Acta* **1979**, *62*, 59.

[13] Lesch, D. A.; Rauchfuss, T. B. *J. Organomet. Chem.* **1980**, *199*, C6.

[14] (a) King, R. B. *J. Am. Chem. Soc.* **1963**, *85*, 1587. (b) Baird, H. W.; White, B. M. *J. Am. Chem. Soc.* **1966**, *88*, 4744.

[15] Wei, C. H.; Dahl, L. F. *Inorg. Chem.* **1965**, *4*, 493.

[16] Bogan, L. E., Jr.; Lesch, D. A.; Rauchfuss, T. B. *J. Organomet. Chem.* **1983**, *250*, 429.

[17] Lesch, D. A.; Rauchfuss, T. B. *Inorg. Chem.* **1983**, *22*, 1854.

[18] Albright, T. A.; Burdett, J. K.; Whangbo, M. H. *Orbital Interactions in Chemistry*; Wiley: New York, 1985; (a) p 82, (b) pp 381–421.

[19] Pauling, L. *The Nature of the Chemical Bond*, 3rd ed.; Cornell University: Ithaca, NY, 1960; p 88.

analogy between the electronic structure and bonding of 8 and the cyclobutadiene analogue $CpCo(C_4H_4)$ diagramed above. Although there are other ways of viewing the $CpCo(\mu\text{-}S)_2Fe_2(CO)_6$ cluster, the isolobality of the near-planar $S_2Fe_2(CO)_6$ moiety and cyclobutadiene, or more precisely $H_2B_2N_2H_2$ (vide infra), is a useful one since it best corresponds to the fragments used in the chemical reaction.

We assume that the reaction yielding 8 occurs by stepwise loss of CO from $(\eta^5\text{-}C_5Me_5)Co(CO)_2$ yielding first $(\eta^5\text{-}C_5Me_5)Co(CO)(\mu\text{-}S)_2Fe_2(CO)_6$ (**9**), which then loses CO to give the observed compound. Although intermediate **9** was not observed we can assign its structure with some confidence as being analogous to those of **3** and **4**, based on the isolobality of $(\eta^5\text{-}C_5H_5)Co(CO)$ and ML_2 (M = Ni, Pd, Pt).[18b] In addition, the rhodium–tellurium analogue $(\eta^5\text{-}C_5H_5)Rh(CO)Te_2Fe_2(CO)_6$ has been reported[17] and was assigned a structure similar to **9** based on spectroscopic evidence and the application of Wade's rules.[20] This rhodium species was found to lose CO to give two species, one of which was proposed to be exactly analogous to **8**. The advantages of describing complexes such as **8** as cyclobutadiene analogues and employing isolobal concepts can be beautifully demonstrated by considering the work of Rauchfuss on the Rh/Te system[17] and our work presented herein. As noted, carbonyl removal from $(\eta^5\text{-}C_5H_5)Rh(CO)Te_2Fe_2(CO)_6$ yielded two isomers.[17] These two isomers are readily explained based on the isolobality of CpM (M = Co, Rh, Ir) and $Fe(CO)_3$;[21] in one case the $(\mu\text{-}Te)_2Fe_2(CO)_6$ moiety functions as the cyclobutadiene-like group which is η^4-bound to CpRh to give a structure analogous to **8**, whereas in the second isomer the cyclobutadiene-like group is $(\mu\text{-}Te)_2Fe(CO)_3RhCp$ which is η^4-bound to $Fe(CO)_3$, analogous to **7**. The isolobal analogy can also be used to explain the subsequent reactions of $CpRh(\mu\text{-}Te)_2Fe_2(CO)_6$ with PPh_3. It is known[22] that nucleophilic attack by PPh_3 on a coordinated cyclobutadiene group can occur, as shown in eq 5, to give a π-allyl species.

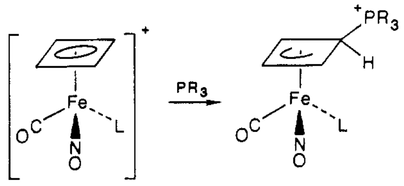

(5)

The two PPh_3 adducts $Fe(CO)_3(PPh_3)(\mu\text{-}Te)_2Fe(CO)_3RhCp$ and $CpRh(PPh_3)(\mu\text{-}Te)_2Fe_2(CO)_6$, described by Rauchfuss,[17] then correspond to PPh_3 adducts of the respective cyclobutadiene-like species, and are themselves π-allyl-like complexes. The structure determination of the sulfide-bridged, triiron analogue $Fe(CO)_3(PPh_3)(\mu\text{-}S)_2Fe_2(CO)_6$,[23] obtained by PPh_3 addition to the cyclobutadiene-like complex $(\mu\text{-}S)_2Fe_3(CO)_9$, confirms the π-allyl formulation for this species, with one $Fe(CO)_3$ moiety η^3-bound to an $S_2Fe(CO)_3$ unit. Noting that the CpRhL, $Fe(CO)_3L$, and ML_2 (M = Ni, Pd, Pt) fragments are all isolobal with CH_2, it also becomes clear that structures **3** and **4** are also π-allyl-like species and can be redrawn as in **10**, to emphasize this point.

Reaction of **1** with $(\eta^5\text{-}C_5H_5)_2Ti(CO)_2$ in benzene at room temperature resulted in the formation of a black, air-stable, benzene-insoluble, high melting (>360 °C) solid whose analysis was in agreement with the formulation $(\eta^5\text{-}C_5H_5)_2Ti(\mu\text{-}S)_2Fe_2(CO)_6$. The insolubility of this species in dichloromethane, methanol, and dimethyl sulfoxide (as well as benzene) precluded NMR spectral investigation or molecular weight determination. One possibility initially considered for its structure was **11**, since the analogous complexes of type **12** are also found to be poorly soluble in organic solvents and have high melting points.[24] However, application of Wade's rules predicts a nido-octahedral structure not unlike those of **7** and **8**. We are currently attempting to obtain crystals of this Ti species in order to establish its structure.

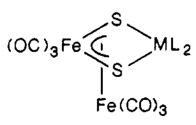

10

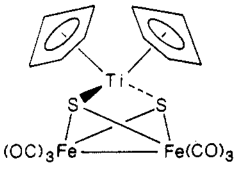

11

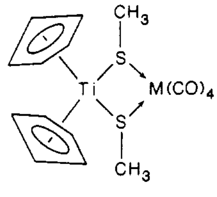

12 (M = Cr, Mo, W)

The reaction of $(\mu\text{-}S_2)Fe_2(CO)_6$ with $[(\eta^5\text{-}C_5Me_5)Co(\mu\text{-}CO)]_2$ (**13**)[25] in toluene solution at 0 °C gave a tetranuclear cluster in 94% yield, which, on the basis of its C, H analysis, IR and ^1H and ^{13}C NMR spectra, and field-desorption mass spectrum, was formulated as $[(\eta^5\text{-}C_5Me_5)Co(\mu\text{-}CO)]_2(\mu\text{-}S)_2Fe_2(CO)_6$ and shown by the X-ray study to have structure **14**. Recalling the isolobality of CpCo(CO) and CH_2, this reaction can be viewed as insertion of the olefin-like species **13** into the S–S bond of **1** to give a π-allyl analogue of **15**. This complex was found to react very slowly at room temperature with 1 molar equiv of $(\mu\text{-}S_2)Fe_2(CO)_6$ to give 2 molar equiv of $(\eta^5\text{-}C_5Me_5)Co(\mu_3\text{-}S)_2Fe_2(CO)_6$.

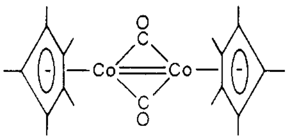

13

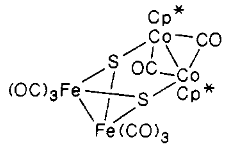

14

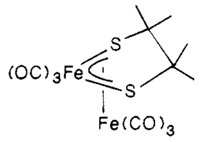

15

We note some other examples of reactions of $(\mu\text{-}S_2)Fe_2(CO)_6$ with metal carbonyls which have been reported since our original preliminary communication[26] on this work. More light has been shed on the $(\mu\text{-}S_2)Fe_2(CO)_6/Co_2(CO)_8$ reaction by Vahrenkamp and co-workers,[27] who found that if this reaction is carried out at 0 °C for 12 h,

---

(20) Wade, K. *Adv. Inorg. Chem. Radiochem.* **1976**, *18*, 1.

(21) Elian, M.; Che, M. M. L.; Mingos, D. M. P.; Hoffmann, R. *Inorg. Chem.* **1976**, *15*, 1148. Hoffmann, R. *Science (Washington, D.C.)* **1981**, *211*, 995. Chinn, J. W., Jr.; Hall, M. B. *Organometallics* **1984**, *3*, 284.

(22) Lukehart, C. M. *Fundamental Transition Metal Organometallic Chemistry*; Brooks/Cole: Monterey, CA, 1985; pp 335–336.

(23) Lesch, D. A.; Rauchfuss, T. B. *Organometallics* **1982**, *1*, 499.

(24) Braterman, P. S.; Wilson, V. A.; Joshi, K. K. *J. Chem. Soc. A* **1971**, 191.

(25) (a) Rausch, M. D.; Genetti, R. A. *J. Org. Chem.* **1970**, *35*, 3888. (b) Bailey, W. I.; Collins, D. M.; Cotton, F. A.; Baldwin, J. C.; Kaska, W. C. *J. Organomet. Chem.* **1979**, *165*, 373.

(26) Seyferth, D.; Henderson, R. S.; Gallagher, M. K. *J. Organomet. Chem.* **1980**, *193*, C75.

(27) Vahrenkamp, H.; Wucherer, E. J. *Angew. Chem., Int. Ed. Engl.* **1981**, *20*, 680.

a tetranuclear cluster, 16, can be isolated in 20–25% yield.

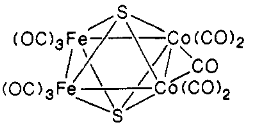

16

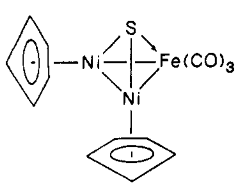

17

Most likely, this is the first product of the reaction which then decomposes at room temperature to give 2. Here again, insertion into the S–S bond of (μ-S_2)$Fe_2(CO)_6$ appears to be the first step. This also appears to be the case in the reaction of (μ-S_2)$Fe_2(CO)_6$ with [(η^5-C_5H_5)Ni(μ-CO)]$_2$ which gave 17 in low yield[28] in a process probably analogous to the (μ-S_2)$Fe_2(CO)_6$/$Co_2(CO)_8$ reaction.

The room temperature reaction of $Fe_2(CO)_9$ with (μ-S_2)$Fe_2(CO)_6$ in THF, which we found gives the known (μ_3-S)$_2Fe_3(CO)_9$ quantitatively, also involves attack at the S–S bond. It is known that $Fe_2(CO)_9$ undergoes cleavage in THF to give $Fe(CO)_5$ and $Fe(CO)_4$(THF),[29] and we suggest that insertion of the latter into the S–S bond of (μ-S_2)$Fe_2(CO)_6$, with subsequent rearrangement and loss of CO, leads to the observed product. Russian workers also have reported formation of (μ_3-S)$_2Fe_3(CO)_9$ in reactions of (μ-S_2)$Fe_2(CO)_6$ with $Fe_2(CO)_9$ and $Fe_3(CO)_{12}$.[30] In our hands (μ-S_2)$Fe_2(CO)_6$ and $Fe(CO)_2(NO)_2$ also reacted in THF to give (μ_3-S)$_2Fe_3(CO)_9$ in 38% yield.

Reactions of (μ-S_2)$Fe_2(CO)_6$, which also appear to proceed initially like that of 15, are those with [(η^5-C_5H_5)Cr(CO)$_3$]$_2$[31] and with [(η^5-C_5H_5)Mo(CO)$_2$]$_2$[32] (the former has a Cr=Cr bond and the latter contains a Mo≡Mo bond). We might have expected the product in the reaction of the Cr complex to be analogous to 14, i.e., resulting from insertion of the double-bonded species into the S–S bond. However, the loss of four carbonyl ligands has occurred, and consequently the coordinative unsaturation has resulted in a rather unusual rearrangement to a closo structure.[31] Similarly, the loss of two carbonyl groups from the Mo complex has resulted in two isomeric closo structures, one of which is analogous to the dichromium product. In both of these reactions the Fe–Fe bond, as well as the S–S bond, of (μ-S_2)$Fe_2(CO)_6$ has been broken to yield the products.

Finally, as we have reported earlier,[33] the reaction of (μ-S_2)$Fe_2(CO)_6$ with $Mn_2(CO)_{10}$, which requires irradiation, presumably to generate (OC)$_5$Mn$^•$ radicals, also involves S–S bond cleavage to give as final product the complex 18.

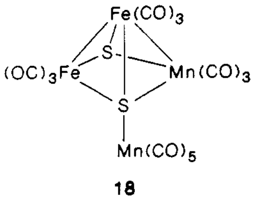

18

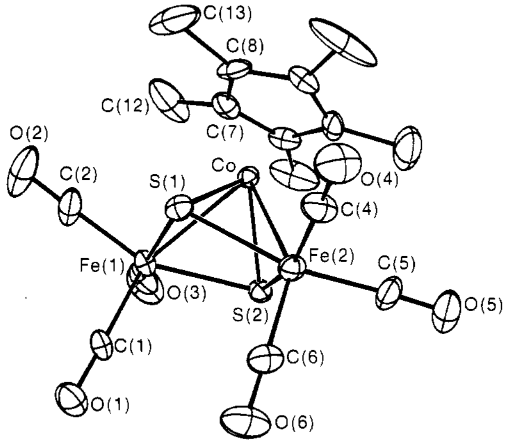

Figure 1. A perspective view of (η^5-C_5Me_5)Co(μ_3-S)$_2Fe_2(CO)_6$ showing the numbering scheme. Carbon atoms on the C_5Me_5 ring are numbered sequentially around the ring, first the ring carbons and then the methyl carbons. Thermal ellipsoids (20%) are diagrammed.

Table I. Selected Distances (Å) in (η^5-C_5Me_5)Co(μ_3-S)$_2Fe_2(CO)_6$[a]

	Bonding Distances		
Co–Fe(1)	2.528 (1)	Fe(1)–S(2)	2.239 (2)
Co–Fe(2)	2.550 (1)	Fe(1)–C(1)	1.787 (9)
Co–S(1)	2.158 (2)	Fe(1)–C(2)	1.778 (10)
Co–S(2)	2.165 (2)	Fe(1)–C(3)	1.788 (8)
Co–C(7)	2.075 (8)	Fe(2)–S(1)	2.237 (2)
Co–C(8)	2.050 (8)	Fe(2)–S(2)	2.233 (2)
Co–C(9)	2.073 (8)	Fe(2)–C(4)	1.803 (9)
Co–C(10)	2.043 (8)	Fe(2)–C(5)	1.809 (11)
Co–C(11)	2.048 (8)	Fe(2)–C(6)	1.777 (10)
Fe(1)–S(1)	2.240 (2)		
	Nonbonding Distances		
Fe(1)–Fe(2)	3.353 (1)	S(1)–S(2)	2.899 (3)

[a] Distances within the carbonyl and pentamethyl cyclopentadienyl groups are given in the supplementary material.

Table II. Selected Angles (deg) in (η^5-C_5Me_5)Co(μ_3-S)$_2Fe_2(CO)_6$[a]

Fe(1)–Co–Fe(2)	82.65 (5)	Co–Fe(2)–S(1)	53.11 (6)
Fe(1)–Co–S(1)	56.44 (6)	Co–Fe(2)–S(2)	53.32 (5)
Fe(1)–Co–S(2)	56.35 (7)	Co–Fe(2)–C(4)	105.0 (3)
Fe(2)–Co–S(1)	55.99 (6)	Co–Fe(2)–C(5)	108.6 (4)
Fe(2)–Co–S(2)	55.82 (6)	Co–Fe(2)–C(6)	142.6 (3)
S(1)–Co–S(2)	84.24 (8)	S(1)–Fe(2)–S(2)	80.88 (8)
Co–Fe(1)–S(1)	53.41 (6)	S(1)–Fe(2)–C(4)	88.3 (3)
Co–Fe(1)–S(2)	53.59 (5)	S(1)–Fe(2)–C(5)	161.4 (4)
Co–Fe(1)–C(1)	144.7 (3)	S(1)–Fe(2)–C(6)	100.0 (3)
Co–Fe(1)–C(2)	104.1 (4)	S(2)–Fe(2)–C(4)	157.9 (3)
Co–Fe(1)–C(3)	105.2 (3)	S(2)–Fe(2)–C(5)	90.3 (3)
S(1)–Fe(1)–S(2)	80.68 (7)	S(2)–Fe(2)–C(6)	102.0 (3)
S(1)–Fe(1)–C(1)	100.5 (3)	S(2)–Fe(2)–C(5)	94.1 (5)
S(1)–Fe(1)–C(2)	90.6 (4)	C(4)–Fe(2)–C(6)	98.8 (4)
S(1)–Fe(1)–C(3)	158.3 (3)	C(5)–Fe(2)–C(6)	97.9 (5)
S(2)–Fe(1)–C(1)	103.9 (3)	Co–S(1)–Fe(1)	70.15 (6)
S(2)–Fe(1)–C(2)	156.8 (3)	Co–S(1)–Fe(2)	70.90 (7)
S(2)–Fe(1)–C(3)	88.9 (3)	Fe(1)–S(1)–Fe(2)	97.02 (8)
C(1)–Fe(1)–C(2)	98.8 (4)	Co–S(2)–Fe(1)	70.06 (7)
C(1)–Fe(1)–C(3)	100.5 (4)	Co–S(2)–Fe(2)	70.86 (6)
C(2)–Fe(1)–C(3)	91.7 (5)	Fe(1)–S(2)–Fe(2)	97.15 (8)

[a] Angles involving the carbonyl and pentamethylcyclopentadienyl groups are given in the supplementary material.

Thus the work reported in this paper, as well as previous work of others, indicates that reactions of (μ-S_2)$Fe_2(CO)_6$ (and the Se and Te analogues) with diverse metal carbonyls and with zerovalent Pd and Pt complexes proceed via initial attack at the S–S bond. This reinforces the close analogy between the reactivity of (μ-S_2)$Fe_2(CO)_6$ and organic disulfides, RSSR. We conclude that the use of iso-

---

(28) Braunstein, P.; Sappa, E.; Tiripicchio, A.; Tiripicchio-Camellini, M. *Inorg. Chim. Acta* **1980**, *45*, L191.

(29) Cotton, F. A.; Troup, J. M. *J. Am. Chem. Soc.* **1974**, *96*, 3438.

(30) (a) Nametkin, N. S.; Tyurin, V. D.; Nekhaev, A. I.; Kukina, M. A. *Izv. Akad. Nauk SSSR, Ser. Khim.* **1985**, 2846. (b) Nametkin, N. S.; Tyurin, V. D.; Kukina, M. A.; Nekhaev, A. I.; Mavlanov, M.; Alekseeva, S. D. *Izv. Akad. Nauk SSSR, Ser. Khim.* **1977**, 2384.

(31) Braunstein, P.; Tiripicchio, A.; Tiripicchio-Camellini, M.; Sappa, E. *Inorg. Chem.* **1981**, *20*, 3586.

(32) (a) Braunstein, P.; Jud, J. M.; Tiripicchio, A.; Tiripicchio-Camellini, M.; Sappa, E. *Angew. Chem., Int. Ed. Engl.* **1982**, *21*, 307. (b) Williams, P. D.; Curtis, M. D.; Duffy, D. N.; Butler, W. M. *Organometallics*, **1983**, *2*, 165.

(33) Seyferth, D.; Henderson, R. S.; Fackler, J. P., Jr.; Mazany, A. M. *J. Organomet. Chem.* **1981**, *213*, C21.

lobal analogies proves to be of great utility in rationalizing some of the chemistry involved.

Molecular Structure of (η^5-C_5Me_5)Co(μ_3-S)$_2$Fe$_2$(CO)$_6$. The unit cell of the compound contains four complex molecules separated by normal van der Waals distances. Figure 1 shows a view of the molecule, and relevant metrical parameters are given in Tables I and II. The structure is one in which the $CoFe_2S_2$ core has a square-pyramidal structure with the two iron and two sulfur atoms forming the base of the pyramid with the cobalt atom at the apex. The geometry around Co can be described as a "four-legged piano stool" with the "legs" being represented by the four bonds to Fe and S. For the most part the "piano stool" is symmetrical, with all angles between adjacent legs of about 56.2°. Another, possibly more chemically useful description of this species is as a sandwich complex in which the Co atom is sandwiched between the C_5Me_5 ring and the four-membered, heteroatom ring of the $S_2Fe_2(CO)_6$ moiety. About both Fe atoms the geometries are approximately octahedral with the three facial carbonyl groups and bonds to Co, S(1), and S(2) comprising the six coordination sites. Distortions from idealized octahedral geometry result because of compression due to binding of the Fe atoms to the CoS_2 moiety; as a result, the angles at the iron atoms, involving Co, S(1), and S(2), are all acute.

The Co–S (average 2.162 (2) Å) and Fe–S (average 2.240 (2) Å)[34] distances are normal and correspond quite closely to those in the related complex (η^5-C_5Me_5)$_2$Co$_2$(μ_3-S)$_2$Fe(NO)$_2$[35] (2.175 (5) and 2.259 (8) Å, respectively). It is interesting that, as in the dinitrosyl complex, the Fe–S bonds are longer than the Co–S bonds; this difference may reflect the different Fe and Co covalent radii.[36] Both Co–Fe distances (2.528 (1) and 2.550 (1) Å) correspond to normal single bonds and are significantly shorter than the analogous distances (2.7571 (4) and 2.8107 (4) Å) in the above dinitrosyl species, in which it was proposed that the average Co–Fe bond orders were less than 1. The Fe–Fe separation, on the other hand (3.353 (1) Å), is long and is clearly outside the accepted range for an Fe–Fe bond.[37] This long Fe–Fe separation results in the Fe(1)–S–Fe(2) angles (average 97.09 (8)°) being much larger than the Co–S–Fe angles (average 70.49 (7)°), in which the sulfur atoms bridge the Co–Fe bonds. The S(1)–S(2) separation (2.899 (3) Å) is also clearly beyond bonding distance[36] and can be contrasted to the S–S bond of 2.007 (5) Å in (μ-S$_2$)Fe$_2$(CO)$_6$ (1).[7] The lengthening of the S–S distance from one which is bonding in 1 to one which is clearly nonbonding in the present compound was anticipated from the apparent reaction of 1 with the (η^5-C_5Me_5)Co fragment. Even the short Fe–Co distances are not unexpected,[16] based on the 18-electron rule. However, the observed structure, in which the Fe–Fe bond has been ruptured, was not expected. It is noteworthy, however, that a similar structure had been proposed for (C_5H_5)Rh(μ-Te)$_2$Fe$_2$(CO)$_6$[17] and an analogous structure had been observed for (μ_3-S)$_2$Fe$_3$(CO)$_9$,[15] in which an Fe(CO)$_3$ moiety replaced the Co(C_5Me_5) group in our complex. (The structural parameters for this triiron species are in close agreement with those of our complex.) The Fe_2S_2 ring in the current species is not exactly planar (see supplementary material) but is puckered slightly with the sulfur atoms lying ca. 0.23 Å above the weighted least-squares plane and the two iron atoms ca. 0.07 Å below this plane. The Fe_2S_2 least-squares plane is almost parallel to the C_5Me_5 plane, with only 1.2° between their normals.

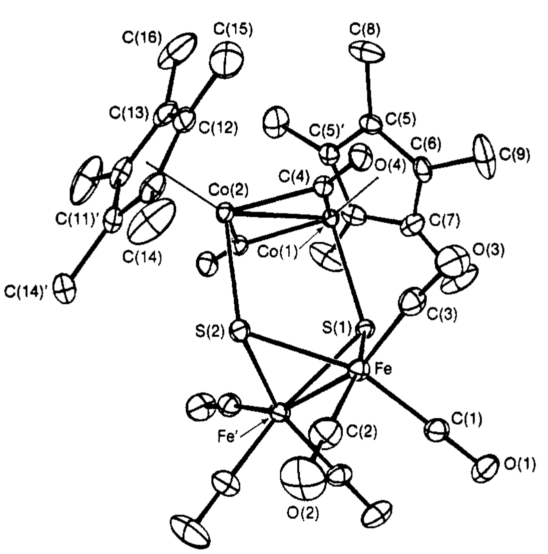

Figure 2. Perspective view of [(η^5-C_5Me_5)Co(μ-CO)]$_2$(μ-S)$_2$Fe$_2$(CO)$_6$ showing the numbering scheme. A crystallographic mirror plane, passing through Co(1), Co(2), S(1), and S(2), bisects the molecule. Primed atoms are related to unprimed ones by this mirror. Thermal ellipsoids (20%) are shown.

Table III. Selected Distances (Å) in [(η^5-C_5Me_5)Co(μ-CO)]$_2$(μ-S)$_2$Fe$_2$(CO)$_6$[a]

Bonding Distances			
Co(1)–Co(2)	2.5084 (7)	Co(2)–C(12)	2.155 (3)
Co(1)–S(1)	2.287 (1)	Co(2)–C(13)	2.140 (5)
Co(1)–C(4)	1.897 (3)	Fe–Fe′	2.4913 (8)
Co(1)–C(5)	2.135 (3)	Fe–S(1)	2.2584 (9)
Co(1)–C(6)	2.116 (3)	Fe–S(2)	2.2628 (9)
Co(1)–C(7)	2.136 (4)	Fe–C(1)	1.788 (3)
Co(2)–S(2)	2.291 (1)	Fe–C(2)	1.772 (4)
Co(2)–C(4)	1.909 (3)	Fe–C(3)	1.788 (4)
Co(2)–C(11)	2.115 (3)		
Nonbonding Distances			
Co(1)–Fe	3.8761 (6)	Co(2)–S(1)	3.565 (1)
Co(2)–Fe	3.8931 (6)	S(1)–S(2)	2.942 (1)
Co(1)–S(2)	3.539 (1)		

[a] Distances within the carbonyl and Cp* groups are given in the supplementary material.

All parameters involving the carbonyl groups appear to be normal, and there is no significant difference between those opposite the Co atom and those opposite the sulfide groups. Similarly the C_5Me_5 ring appears normal; the rather narrow range in Co–C distances (2.043 (8)–2.075 (8) Å) indicates that the C_5Me_5 ring is symmetrically bound. The elongated thermal ellipsoids of this group are typical of such groups displaying significant librational motion about the metal–Cp* group axis.

Molecular Structure of [(η^5-C_5Me_5)Co(μ-CO)]$_2$(μ-S)$_2$Fe$_2$(CO)$_6$. This complex, shown in Figure 2, crystallizes in the space group $P2_1/m$ with two molecules in the cell, occupying the special positions of symmetry m. As a consequence the complex has crystallographically imposed mirror symmetry, with the mirror plane containing the two

---

[34] The esd shown for an average quantity is the largest esd of the numbers from which the average is calculated.

[35] Seyferth, D.; Gallagher, M. K.; Cowie, M. *Organometallics* **1986**, *5*, 539.

[36] The relevant Pauling covalent radii are as follows: Co, 1.16 Å; Fe, 1.17 Å; S, 1.02 Å. It must also be kept in mind that the Co and Fe atoms have different oxidation states in this compound.

[37] Normal Fe–Fe single bonds lie in the range 2.485 (1)–2.747 (1) Å (see: Chu, C. T.-W.; Dahl, L. F. *Inorg. Chem.* **1977**, *12*, 3245. Clegg, W. *Inorg. Chem.* **1976**, *15*, 2928. Seyferth, D.; Womack, G. B.; Song, L.-C.; Cowie, M.; Hames, B. W. *Organometallics* **1983**, *2*, 928. Seyferth, D.; Womack, G. B.; Cowie, M.; Hames, B. W. *Organometallics* **1983**, *2*, 1696. References 27–29). However, very long Fe–Fe bonds (up to 3.089 (7) Å) have been observed when large bridging groups force the metals apart (see: Dahl, L. F.; deGil, E. R.; Feltham, R. D. *J. Am. Chem. Soc.* **1969**, *91*, 1653).

Table IV. Selected Angles (deg) in $[(\eta^5\text{-}C_5Me_5)Co(\mu\text{-}CO)]_2(\mu\text{-}S)_2Fe_2(CO)_6$[a]

Co(2)–Co(1)–S(1)	95.94 (3)	S(1)–Fe–C(2)	156.7 (1)
Co(2)–Co(1)–C(4)	48.97 (8)	S(1)–Fe–C(3)	106.9 (1)
S(1)–Co(1)–C(4)	93.06 (9)	S(2)–Fe–C(1)	154.0 (1)
Co(1)–Co(2)–S(2)	94.93 (3)	S(2)–Fe–C(2)	87.8 (1)
Co(1)–Co(2)–C(4)	48.58 (8)	S(2)–Fe–C(3)	110.7 (1)
S(2)–Co(2)–C(4)	92.42 (9)	C(1)–Fe–C(2)	93.4 (2)
Fe′–Fe–S(1)	56.53 (2)	C(1)–Fe–C(3)	95.1 (2)
Fe′–Fe–S(2)	56.60 (2)	C(2)–Fe–C(3)	96.2 (2)
Fe′–Fe–C(1)	97.7 (1)	Co(1)–S(1)–Fe	117.04 (4)
Fe′–Fe–C(2)	100.3 (1)	Fe–S(1)–Fe′	66.95 (3)
Fe′–Fe–C(3)	158.4 (1)	Co(2)–S(2)–Fe	117.54 (4)
S(1)–Fe–S(2)	81.19 (3)	Fe–S(2)–Fe′	66.81 (4)
S(1)–Fe–C(1)	87.7 (1)		

[a] Angles involving the carbonyl and Cp* groups are given in the supplementary material.

Co and two S atoms and perpendicular to the Fe–Fe bond. Metrical parameters for the complex are given in Tables III and IV. The structure can be thought of as being derived from insertion of the $[(\eta^5\text{-}C_5Me_5)Co(\mu\text{-}CO)]_2$ group into the S–S bond of the $(\mu\text{-}S_2)Fe_2(CO)_6$ "butterfly", such that the product has the Co(1)–Co(2) bond lying essentially parallel to the S(1)–S(2) vector which is in turn perpendicular to the Fe–Fe′ bond. This product is essentially that expected from the insertion of the unsaturated Co_2 fragment into the S–S bond of the Fe_2S_2 butterfly and contrasts to the product described in the previous section, in which insertion of $(\eta^5\text{-}C_5Me_5)Co$ into the S–S bond was accompanied by the formation of Co–Fe bonds. The very long Co–Fe separations (3.8761 (6)–3.8931 (6) Å) in the present compound are clearly outside of normal bonding limits and indicate the absence of such bonding. On the other hand, the Co(1)–Co(2) and Fe–Fe′ distances (2.5084 (7) and 2.4913 (8) Å, respectively) correspond to normal single bonds, showing that both bonds have remained intact. The Co–Co separation has lengthened significantly from the value of 2.327 (2) Å observed in the precursor $[(\eta^5\text{-}C_5Me_5)Co(\mu\text{-}CO)]_2$,[25b] consistent with a change in Co–Co bond order from 2 to 1 upon reaction.

Within the Fe_2S_2 butterfly part of the molecule the parameters are essentially as expected, comparing well with other related species.[38-40] Both Fe–S distances (2.2584 (9) and 2.2628 (9) Å) are in good mutual agreement and are consistent with previous determinations. The S(1)–S(2) separation of 2.942 (1) Å is beyond bonding distance and is comparable to that observed in $(\mu\text{-}C_2H_5S)_2Fe_2(CO)_6$ (2.93 (1) Å),[38] in which the two sulfur atoms are not linked, but is significantly larger than the values of 2.662 (3) and 2.673 (2) Å observed in $[\mu\text{-}CH_3C(O)CH_2CHS_2]Fe_2(CO)_6$[39] and $(\mu\text{-}CH_2S_2)Fe_2(CO)_6$,[40] respectively, in which the two sulfur atoms are linked by one-carbon-atom bridges. The dihedral angle between the two Fe–S–Fe′ planes in the present structure is 102.48 (4)°.

The $[(\eta^5\text{-}C_5Me_5)Co(\mu\text{-}CO)]_2$ moiety is connected to the $(\mu\text{-}S)_2Fe_2(CO)_6$ fragment by only the two cobalt–sulfide linkages to give two metal–metal bonded Co(II) centers. The resulting Co–S bonds (2.287 (1) and 2.291 (1) Å) are normal, although they are slightly longer than those noted earlier for analogous molecules. It may be that steric interactions between the "Co_2" and "Fe_2" halves of the molecule weaken the Co–S linkages somewhat. Oxidative addition of this Co_2 dimer across the S–S bond has resulted in rather few changes in the structure of this dimer. In addition to the lengthening of the Co–Co bond as alluded to earlier, the C_5Me_5 rings have also bent back away from the Co–S linkages; in the starting Co_2 dimer these groups were perpendicular to the Co=Co bond. Surprisingly perhaps, the bridging carbonyl groups remain coplanar with the two Co centers, instead of folding slightly about the Co(1)–Co(2) bond. The geometries of these bridging carbonyl groups are normal, and similarly the C_5Me_5 groups are unexceptional.

The two structures described in this paper illustrate two ways in which unsaturated metal fragments can oxidatively add to the $(\mu\text{-}S_2)Fe_2(CO)_6$ complex. Although it seems that initial reaction in each case occurs at the S–S bond, the greater coordinative unsaturation of the $(\eta^5\text{-}C_5Me_5)Co$ fragment compared to the $((\eta^5\text{-}C_5Me_5)Co(\mu\text{-}CO))_2$ dimer necessitates additional Co–Fe bond formation in the reaction of the former.

Electronic Structure and Bonding. The isolobal analogy provides a simple rationalization of the structure of $(\eta^5\text{-}C_5Me_5)Co(\mu_3\text{-}S_2)Fe_2(CO)_6$, which is reminiscent of substituted cyclobutadiene complexes of cobalt[41-43] and rhodium,[44,45] with the cyclic $S_2Fe_2(CO)_6$ moiety substituting for the cyclobutadiene ring. In fact, this moiety and a $(POR)_2Fe_2(CO)_6$ complex[46] are both isolobal with cyclobutadiene, as first proposed[47] for the POR compound and confirmed by our theoretical studies on $S_2Fe_2(CO)_6$ (vide infra). The observed structures of $(\eta^5\text{-}C_5Me_5)Co(\mu_3\text{-}S)_2Fe_2(CO)_6$, $(\mu_3\text{-}S)_2Fe_3(CO)_9$,[15] $[Fe_3(CO)_9(\mu_3\text{-}PMes)_2]\cdot THF$,[47] and $Fe(CO)_3(\eta^4\text{-}C_4H_4)$[48] are very analogous, providing further support for the isolobal analogy. The isolobality of $Fe(CO)_3$ and CpCo is well-known.[21]

We will return to the isolobal analogy later, but first we discuss the interaction of the frontier orbitals of CpCo and of $(\mu\text{-}S_2)Fe_2(CO)_6$. Considering each of these fragments as neutral moieties, the Co atom achieves a complement of only 14 electrons whereas each Fe atom achieves the magic number of 18. (The CpCo fragment is treated formally as Cp^- and Co^+, so that the Co atom has eight valence electrons.) Although the local symmetry of the CpCo group is C_{5v}, we will consider its frontier orbitals in terms of C_{2v} so as to have common symmetry labels between the two fragments. Since the frontier orbitals of CpCo are localized on the Co end of the fragment, it is immaterial that the Cp ring orbitals do not transform as C_{2v}.

The main point of the calculations to be presented in this section is to examine the evolution of the frontier orbitals of $(\mu\text{-}S_2)Fe_2(CO)_6$ as a function of the dihedral angle between the two Fe_2S planes. As mentioned in the introduction, this is best done for three dihedral angles: 65°, 95°, and 156°. In the first the Fe_2S_2 cluster has both its Fe–Fe and S–S bonds, in the second the S–S bond is broken, and in the last both the S–S and Fe–Fe bonds have been broken. For the 95° and 156° structures we will examine the nature of the frontier orbitals and how these interact with an incoming group, such as GeH_2, which

---

(38) Dahl, L. F.; Wei, C.-H. *Inorg. Chem.* **1963**, *2*, 328.

(39) Seyferth, D.; Womack, G. B.; Henderson, R. S.; Cowie, M.; Hames, B. W. *Organometallics* **1986**, *5*, 1568.

(40) Shaver, A.; Fitzpatrick, P. J.; Steliou, K.; Butler, I. S. *J. Am. Chem. Soc.* **1974**, *101*, 1313.

(41) Bruce, R.; Maitlis, P. M. *Can. J. Chem.* **1967**, *45*, 2017.

(42) Härter, P.; Pfisterer, H.; Ziegler, M. L. *Angew. Chem., Int. Ed. Engl.* **1986**, *25*, 839.

(43) Debaerdemaeker, T.; Grafl, D.; Brune, H. A. *Acta Crystallogr., Sect. C: Cryst. Struct. Commun.* **1987**, *C43*, 221.

(44) Cash, G. G.; Helling, J. F.; Mathew, M.; Palenik, G. J. *J. Organomet. Chem.* **1973**, *50*, 277.

(45) Reisner, G. M.; Bernal, I.; Rausch, M. D.; Gardner, S. A.; Clearfield, A. *J. Organomet. Chem.* **1980**, *184*, 237.

(46) Flynn, K. M.; Bartlett, R. A.; Olmstead, M M.; Power, P. P. *Organometallics* **1986**, *5*, 813.

(47) Bartlett, R. A.; Rasika Dias, H. V.; Flynn, K. M.; Olmstead, M. M.; Power, P. P. *J. Am. Chem. Soc.*, in press.

(48) For leading references to structural studies see: Chinn, J. W., Jr.; Hall, M. B. *Inorg. Chem.* **1983**, *22*, 2759.

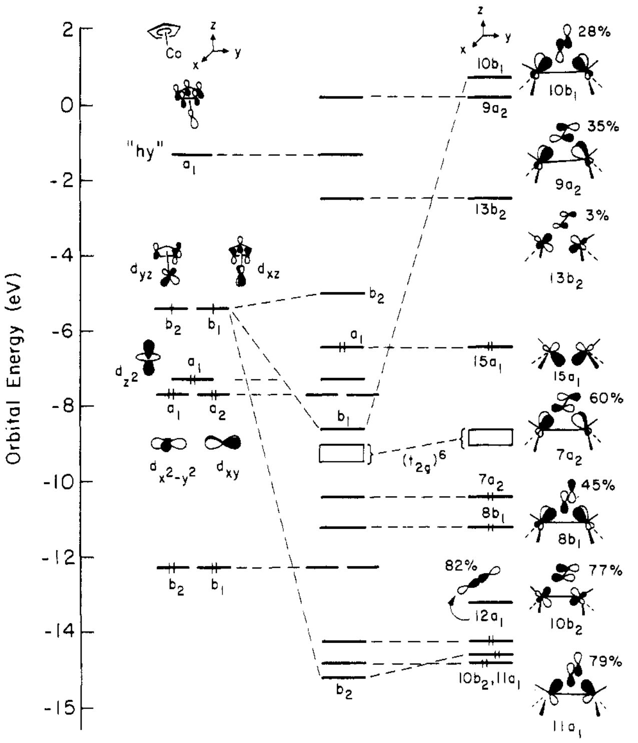

Figure 3. Schematic orbital interaction diagram between the CpCo and $(\mu_2\text{-}S_2)Fe_2(CO)_6$ fragments with the latter fragment in its original configuration with an S–S bond length of 2.0 Å. The group of orbitals labeled $(t_{2g})^6$ actually contains 12 electrons, six from each of the Fe atoms. The Fe d orbitals are sketched only qualitatively. For example, the $8b_1$ fragment orbital is mainly d_{xy} character, and $7a_2$ is mainly d_{xz} character.

needs only two more electrons to achieve its complement of electrons (octet). The CpCo group, on the other hand, needs four electrons to achieve the 18-electron rule, and this can only be achieved in the 156° structure. These details will become clear as we examine the frontier orbitals in each of the configurations.

a. 65° Configuration. Figure 3 presents the frontier orbitals of both fragments along with sketches of the nature of these orbitals, as obtained from the Fenske–Hall calculations. In addition, we sketch in qualitative interactions between the fragment orbitals while the $(\mu\text{-}S_2)Fe_2(CO)_6$ fragment is maintained in its initial geometrical configuration. (We retain the same orbital numbering system as was employed in our earlier work.[5b,c])

It is clear that the frontier orbital interaction is not very suitable, as illustrated by considering the a_1 representation. The $15a_1$ orbital of $(\mu\text{-}S_2)Fe_2(CO)_6$, although of the correct symmetry to interact with "hy" of CpCo, does not present a good overlap match. This orbital is a bent Fe–Fe bond, pointing *away from* the S_2 fragment. There also are two a_1 orbitals among the 12 electrons derived from the "nonbonding" $(t_{2g})^6$ set on each of the two iron atoms. These will not be well disposed to interact with the incoming CpCo moiety because the S_2 group is interfering with a near-neighbor interaction. In addition, there are a pair of sulfur-based MOs ($11a_1$ and $12a_1$) which can donate electrons into the empty "hy" orbital of CpCo but which are energetically so stable as to hardly be classified as frontier orbitals. (These orbitals ionize at about 12.4 eV in the gas-phase photoelectron spectrum.[5c,49]) In summary, the a_1 interactions are not very conducive to bonding between the fragments. Since this is the highest symmetry representation, it is unlikely that significant improvement will occur by invoking bonding in other symmetries. Nonetheless, we will briefly mention what is found in those cases.

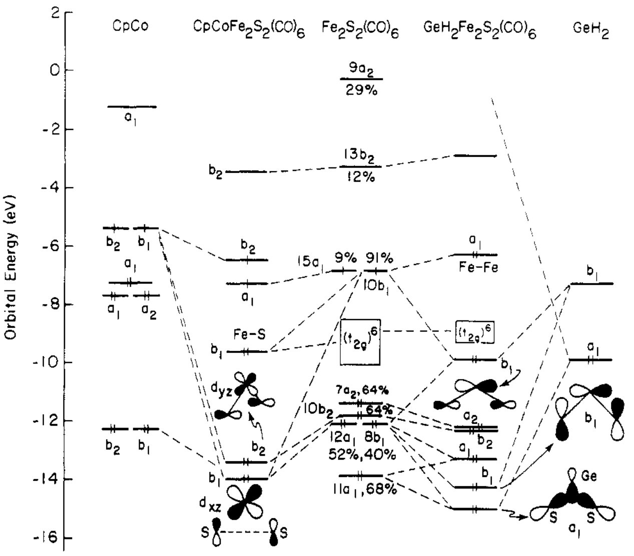

Figure 4. Orbital interaction diagram for $CpCoFe_2S_2(CO)_6$ and $GeH_2Fe_2S_2(CO)_6$. The $(\mu_2\text{-}S)_2Fe_2(CO)_6$ fragment has an S–S bond length of 2.77 Å and a dihedral angle of $\theta = 95°$. The percentage numbers written next to these fragment orbitals refer to the amount of sulfur character in these fragment MOs. The major orientation of these S orbitals can be determined by references to Figure 3. Since we were unable to achieve a satisfactory SCF convergence for the $CpCoFe_2S_2(CO)_6$ molecule, we provide only partial results for this calculation.

The $(\mu\text{-}S_2)Fe_2(CO)_6$ fragment presents a set of three low-lying empty orbitals labeled $10b_1$, $9a_2$, and $13b_2$. The latter has only about 3% S character (9% in the Hartree–Fock–Slater work[5b]) which will give a little interaction with the corresponding d_{yz} orbital of CpCo. Its bonding counterpart, $10b_2$, will be able to interact with the d_{yz} orbital, but the energy mismatch is quite severe. Meanwhile, the empty $10b_1$ orbital of $(\mu\text{-}S_2)Fe_2(CO)_6$ can interact strongly with the d_{xz} orbital of CpCo. The Δ interaction in the a_2 representation is expected to provide little bonding. The LUMO b_2 orbital (mainly Co d_{yz}) is at very low-lying energy, indicative of the fact that the Co atom has achieved an electron count of only 16 instead of the "desired" 18.

In summary, we see from Figure 3 that there will be only four electrons to provide bonding between the two fragments. While this interaction is expected to be weak, it will weaken and lengthen the S–S bond, since depopulating $10b_2$ and populating $10b_1$ will have this effect as seen from the orbital character depicted in Figure 3. This discussion then leads us naturally to the second structure to be discussed which has a broken S–S bond.

b. 95° Configuration. In Figure 4 we present the frontier orbitals of a $(\mu\text{-}S_2)Fe_2(CO)_6$ fragment with a dihedral angle (θ) of 95° between the two Fe_2S planes. This model fragment has the same assumed Fe–S bond length as the parent compound, but the S–S bond length has been lengthened from 2.0 to 2.77 Å. The frontier orbitals of $(\mu\text{-}S_2)Fe_2(CO)_6$ in the original $\theta = 65°$ and the present $\theta = 95°$ configuration differ mainly in the dramatic lowering in energy of the $10b_1$ fragment orbital. (This was also evident in our earlier work on the dianion.[5b]) Since this orbital is S_2 π^*, it is not surprising that it is stabilized upon stretching the S–S bond. The "$(t_{2g})^6$" orbitals are not

---

(49) Andersen, E. L.; Fehlner, T. P.; Foti, A. E.; Salahub, D. R. *J. Am. Chem. Soc.* **1980**, *102*, 7422. Van Dam, H.; Louwen, J. N.; Oskam, A.; Doram, N.; Hillier, I. H. *J. Electron Spectrosc. Relat. Phenom.* **1980**, *21*, 57.

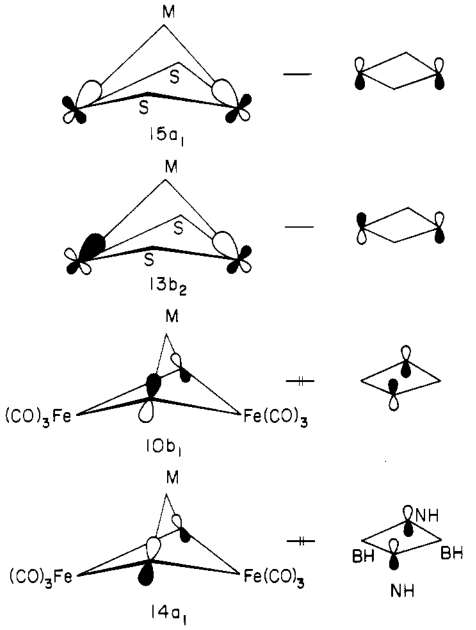

Figure 5. Predominant character of the four frontier orbitals for $(\mu_2\text{-S})_2Fe_2(CO)_6$ and a qualitative set of the corresponding orbitals for $H_2B_2N_2H_2$. The horizontal lines are meant to show which of the frontier orbitals are occupied in the iron–sulfur moiety. The location of atom "M" is shown only to indicate the position of an incoming Ge or Co atom.

nearly so "pure" as they were in Figure 3. These MOs contain a significant fraction of S character, just as we found in our studies on the dianion.[5b] The orientation of the S orbital character (indicated by percent) can be seen by reference to the corresponding orbitals in Figure 3. Also presented in Figure 4 are the frontier orbitals of CpCo and GeH_2 and the calculated orbital energies for the resultant complexes.

We first draw attention to the MO diagram for $GeH_2(\mu_3\text{-S})_2Fe_2(CO)_6$ and notice that there is strong interaction of fragment a_1 and b_1 orbitals. Each fragment contributes two electrons to the formation of two new Ge–S bonds. (The two b_1 MOs that are sketched provide essentially one Ge–S bond.) Furthermore, there is a large HOMO–LUMO gap and the $(t_{2g})^6$ orbitals become much more pure. All of these features point to the formation of a stable molecular complex.

In contrast to the above description of the GeH_2 complex, the MO diagram for this "θ = 95°" structure of $CpCo(\mu_3\text{-S})_2Fe_2(CO)_6$ presents distinct problems. There is interaction in both the b_1 and b_2 representations, but the $15a_1$ orbital does not interact at all well with "hy" of CpCo, mainly because there is only 9% S character on this frontier orbital. As a result of the relatively poor correlation diagram, there is a small HOMO–LUMO gap and we are unable to achieve SCF convergence to a closed-shell singlet.[50]

c. 156° Configuration. We turn next to Figure 5 which displays the four most important frontier orbitals of $(\mu_2\text{-S})_2Fe_2(CO)_6$ in the θ = 156.3° configuration, as it is found in the crystallographic work presented earlier for $(\eta^5\text{-}C_5Me_5)Co(\mu_3\text{-S})_2Fe_2(CO)_6$. Also shown in Figure 5 are qualitative sketches of the corresponding four frontier orbitals of $H_2B_2N_2H_2$, a molecule that is isoelectronic with cyclobutadiene. We see immediately that these two moieties are indeed isolobal. It is easy to see how these orbitals for the $(\mu_2\text{-S})_2Fe_2(CO)_6$ fragment in its θ = 156.3° configuration evolve from the θ = 95° case; the antibonding Fe–Fe orbital ($13b_2$) is strongly stabilized due to lengthening of the Fe–Fe bond. Meanwhile, the $15a_1$ orbital (Fe–Fe bonding) is destabilized for the same reason. This change in nature of the frontier orbitals will have a dramatic effect on the interaction with incoming CpCo and GeH_2 fragment orbitals.

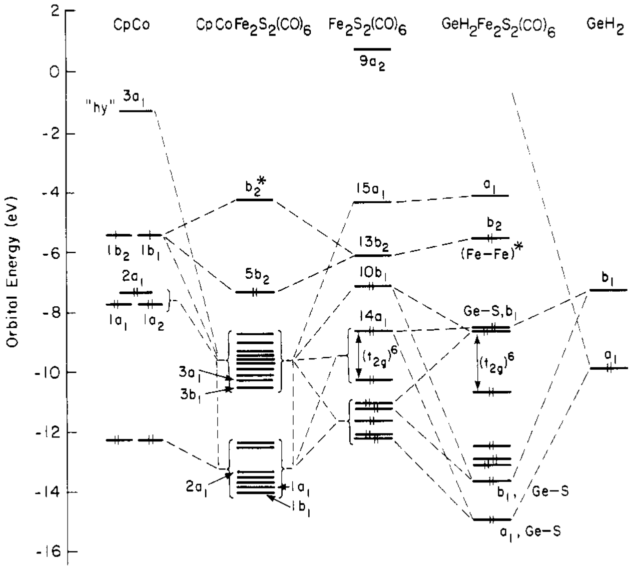

Figure 6. Orbital interaction diagram for $CpCoFe_2S_2(CO)_6$ and $GeH_2Fe_2S_2(CO)_6$. The $(\mu_2\text{-S})_2Fe_2(CO)_6$ fragment has a dihedral angle of θ = 156.3°. The only correlation lines that have been drawn are those pertinent to the discussion.

In Figure 6 we display an eigenvalue spectrum for the frontier orbitals of $(\mu_2\text{-S})_2Fe_2(CO)_6$ (θ = 156.3°) along with those for CpCo and GeH_2 and show the resultant eigenvalues for the complexes of these moieties with the iron–sulfur fragment. The situation is just reversed compared to Figure 4. Now it is the GeH_2 complex that has poor interactions and a small HOMO–LUMO gap whereas the CpCo complex has strong interactions among fragment orbitals and a large HOMO–LUMO gap. We take up these relatively complicated MO diagrams one at a time to show that they make eminent sense at a qualitative level.

Turning first to the diagram for $GeH_2Fe_2S_2(CO)_6$ we see that there are strong Ge–S interactions in both the a_1 and b_1 representations, just as shown in Figure 4. However, the HOMO b_2 orbital contains a pair of Fe–Fe anti-bonding electrons and hence these electrons are "wasted" as far as their contribution to holding the complex together. With only four electrons available for a potential of four bonds (two Ge–S and two Fe–S) the situation does not look good. Indeed, use of a simple Lewis electron dot structure would allow one to predict that this configuration is unstable for the GeH_2 complex.

The MO diagram for the $CpCo(\mu_3\text{-S})_2Fe_2(CO)_6$ complex is quite different. As mentioned above, the interactions are strong and there is a large HOMO–LUMO gap, all indicative of stability for this known complex. In Figure 6 the uppermost 18 occupied orbitals for this complex are shown. They divide themselves into three groups in the energy spectrum: a group of seven MOs between −12 and −14 eV, a second group of ten MOs between −8.5 and −10.5 eV, and the HOMO at −7.35 eV. The first group of seven MOs are correlated as follows: two from π Cp and five from metal–sulfur bonds. The sixth metal–sulfur bond is at the bottom of the second group ($3b_1$). It is destabilized because of its σ^* S_2 character (see **19**). The second group of nine MOs (not ten since we have just discussed $3b_1$), plus

---

[50] The results displayed in Figure 3 for $CpCoFe_2S_2(CO)_6$ were actually converged with 1.5 electrons in each of the four upper occupied MOs.

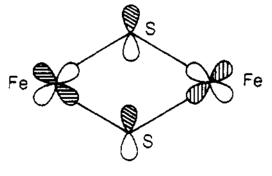

19

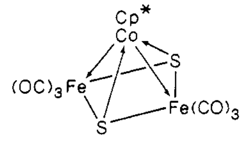

20

the HOMO, can be ascribed to the mainly d electrons on the metals. There are eight electrons associated with the cobalt atom and a set of "$(t_{2g})^6$" associated with each iron atom. (The other two electrons from each Fe atom have already been utilized in forming the Fe–S bonds.) The HOMO is split out from the other nine MOs due to its nodal character (b_2) and the fact that the fragment orbitals from which it is derived are high in energy. This short description provides an overview of the bonding which can be summarized with the simple Lewis electron dot diagram (**20**), a simple picture that can be sustained by a more detailed examination of the MOs.

In order to distill the essence from the MO diagram in Figure 6 we examined the Mulliken population analysis of the fragment orbitals in the molecule. Only four orbitals from each fragment has a population significantly less than 2.0 and more than 0.0 electrons. These fragment orbitals and their populations are given in Table V, along with the values of the important overlap integrals between these fragment orbitals.

In Figure 7 are sketched the qualitative nature of these fragment orbitals showing their interaction in the MOs of $CpCo(\mu_3\text{-}S)_2Fe_2(CO)_6$. Roughly speaking, there is S→Co donation in MOs $1b_1$, $1a_1$, and $2a_1$ whereas the Co→Fe donation occurs in MOs $3a_1$ and $5b_2$.

In Table VI are provided the calculated Mulliken atomic charges of the free and bound fragments for $CpCo(\mu_3\text{-}S)_2Fe_2(CO)_6$. Also shown are the Mulliken atomic charges for the Fe and S atoms in "normal" ($\theta = 65°$) $(\mu\text{-}S_2)Fe_2(CO)_6$. The comparison of the atomic charges in the $\theta = 65°$ and $\theta = 156°$ configurations show that the charge is much more polarized in the latter, with the Fe atoms becoming more positive and the S atoms becoming more negative than in the parent molecule ($\theta = 65°$). This indicates that the Fe atoms are prepared to accept electron density from the CpCo moiety and the S atoms are prepared to donate electrons. This concept is indicated in the Lewis electron dot structure and by the change in computed atomic charges upon formation of the compound (Table VI). The Co atomic charge is barely changed upon complex formation.

Experimental Section

General Comments. All reactions were carried out under an atmosphere of prepurified nitrogen unless otherwise indicated. Air and/or moisture-sensitive materials were handled either in a Vacuum Atmospheres HE-43 Dri-Lab glovebox or by using standard Schlenk techniques. Benzene, toluene, and tetrahydrofuran (THF) were purified by distillation from potassium or sodium/benzophenone ketyl under a nitrogen atmosphere. Similarly, pentane, hexane, and diethyl ether were purified by distillation from lithium aluminum hydride under a nitrogen atmosphere. All other solvents were of reagent grade and used without further purification unless oxygen-free solvent was needed; then the solvent was purged with nitrogen for ca. 15 min. Thin-layer chromatography (TLC) was used where possible to monitor the progress of the reaction being studied (J.T. Baker silica gel plates) and column or filtration chromatography was used to isolate the desired product using silicic acid as the support (Mallinckrodt reagent, 100 mesh). Air-sensitive compounds were chromatographed under nitrogen by using Florisil (Fisher reagent, 100 mesh) as the support. The colors of the compound made visualization of the chromatographs straightforward.

Table V. Mulliken Occupancy of Fragment Orbitals in the Complex $CpCo(\mu_3\text{-}S)_2Fe_2(CO)_6$ and the Pertinent Overlap Integrals

CpCo		$(\mu_2\text{-}S)_2Fe_2(CO)_6$		⟨MO(1)|-MO(2)⟩
MO(1)	occupatn	MO(2)	occupatn	
$1a_1$	1.83	$15a_1$	0.20	0.096
$3a_1$	0.37	$14a_1$	1.89	0.348
$1b_2$	1.04	$13b_2$	1.02	0.169
$1b_1$	0.71	$10b_1$	1.32	0.224

Table VI. Calculated Mulliken Charges

	fragment				
molecule	Fe	S	CO (av)	Co	Cp
$Fe_2S_2(CO)_6$ ($\theta = 65°$)	0.04	–0.04	0.00		
$Fe_2S_2(CO)_6$ ($\theta = 156.3°$)	0.28	–0.51	0.08		
CpCo				0.62	–0.62
$CpCoFe_2S_2(CO)_6$	0.11	–0.35	0.06	0.56	–0.45

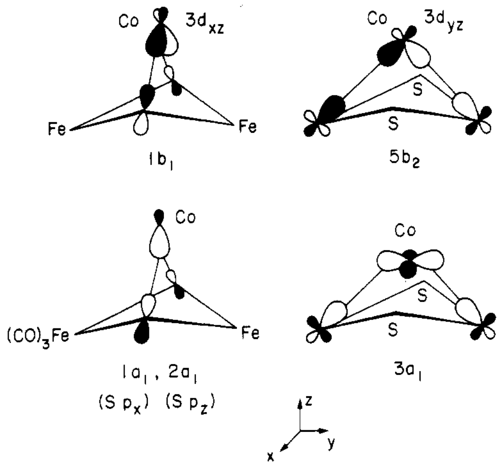

Figure 7. Schematic diagram showing the major MOs that are important in bonding the CpCo fragment to the $(\mu_2\text{-}S)_2Fe_2(CO)_6$ fragment.

Proton nuclear magnetic resonance spectra were recorded at 60 MHz on a Varian Associates T-60 or a Hitachi-Perkin Elmer R-20B spectrometer. High-field proton NMR spectra were recorded at 250 MHz on a Bruker WM-250 operating in the Fourier transform mode. Chemical shifts are reported in δ units, parts per million downfield from internal tetramethylsilane or using the solvent as the reference signal. Carbon-13 NMR spectra were recorded on a JEOL FX-90 operating at 15 MHz or a Bruker WM-270 operating at 67.9 MHz in the Fourier transform mode. Infrared spectra were obtained by using a Perkin-Elmer 457A or 1430 double-beam grating spectrometer. Solution samples were contained in 0.1-mm path-length sodium chloride solution cells. EI Mass spectra were recorded on a Varian MAT 44 or a Finnigan 3200 mass spectrometer operating at 70 eV. Field desorption mass spectra were recorded on a Finnigan MAT 731 mass spectrometer operating in the positive ion mode. Melting points were determined by using analytically pure samples, which were sealed in evacuated or nitrogen-filled capillaries, on a Büchi melting point apparatus and are uncorrected. Microanalyses were performed by Scandinavian Microanalytical Laboratories, Herlev, Denmark. Samples were sent sealed in evacuated or nitrogen-filled vials.

Starting materials were either purchased or prepared by using literature procedures: $(\mu\text{-}S_2)Fe_2(CO)_6$,[51] $(\eta^5\text{-}C_5H_5)Co(CO)_2$,[52] $(\eta^5\text{-}C_5Me_5)Co(CO)_2$,[25] $[(\eta^5\text{-}C_5Me_5)Co(\mu\text{-}CO)]_2$,[25] $(\eta^5\text{-}C_5H_5)_2Ti(CO)_2$.[53]

Reaction between (μ-Dithio)bis(tricarbonyliron) and Tetrakis(triphenylphosphine)platinum(0) in the Presence

---

(51) (a) Brendel, G. Dissertation, Technische Hochschule München, 1956. (b) Hieber, W.; Gruber, J. *Z. Anorg. Allg. Chem.* **1958**, *296*, 91.

(52) Eisch, J. J.; King, R. B. *Organometallic Syntheses*; Academic: New York, 1965; Vol. 1, p 115.

(53) Thomas, J. L.; Brown, K. T. *J. Organomet. Chem.* **1976**, *111*, 297.

of Methyl Iodide. A 100-mL round-bottomed flask fitted with a serum cap was charged with 0.344 g (1.00 mmol) of $(\mu\text{-}S_2)Fe_2(CO)_6$ and flushed with nitrogen. Next, 50 mL of benzene and 2.5 mL (an excess) of CH_3I (Aldrich) were added. (If CH_3I was not added, TLC showed the presence of many products. Probably this was due to a reaction between the liberated PPh_3 and $(\mu\text{-}S_2)Fe_2(CO)_6$.) In a drybox, a 200-mL round-bottomed flask equipped with a magnetic stir-bar, a serum cap, and a nitrogen inlet needle was charged with 0.488 g (0.392 mmol) of $(PPh_3)_4Pt$ (Strem). The former solution was cannulated into this reaction vessel. After the reaction mixture had been stirred for 1 h, a white precipitate ($[Ph_3PCH_3]I$—not quantified) was present in the orange-red reaction mixture. After filtration, solvent was removed from the filtrate on a rotary evaporator, leaving a red solid which was chromatographed on silicic acid. Pentane eluted an orange band which yielded a trace of $(\mu\text{-}S_2)Fe_2(CO)_6$. Dichloromethane eluted a red band which, upon removal of solvent, gave 0.412 g (0.388 mmol, 99% yield) of $[\mu\text{-}(Ph_3P)_2PtS_2]Fe_2(CO)_6$ as an orange-red, crystalline solid which was recrystallized from CH_2Cl_2/pentane; mp 200 °C dec. IR (CH_2Cl_2): 1481 w, 1435 v, 1096 m, 1002 w, 803 w, 610 m cm^{-1}. Terminal carbonyl region: 2050 s, 2009 vs, 1972 s, 1959 s cm^{-1}. ^1H NMR ($CDCl_3$): δ 7.13–7.56 (m, $-PPh_3$, br). ^{31}P NMR (THF): δ_P 19.7 [s with Pt satellites, $J(^{195}Pt-^{31}P)$ = 2795 Hz]. Anal. Calcd for $C_{42}H_{30}Fe_2O_6P_2PtS_2$: C, 47.43; H, 2.84. Found: C, 47.25; H, 2.88.

Reaction between (μ-Dithio)bis(tricarbonyliron) and Tetrakis(triphenylphosphine)palladium(0) in the Presence of Methyl Iodide. A 200-mL round-bottomed flask equipped with a stir-bar, a serum cap, and a nitrogen inlet needle was charged with 0.605 g (0.523 mmol) of $(PPh_3)_4Pd$ (Strem). Benzene (30 mL) was added, and the solution was stirred for approximately 6 min while the solution was purged with CO. (This method converts the insoluble L_4Pd to the soluble $L_3Pd(CO)$.[12]) At this point the solution became homogenous and 3.0 mL (an excess) of CH_3I was added. The CO purge was continued for an additional 15 min, after which time the solution was orangish and contained a white precipitate. In the meantime, a 100-mL flask fitted with a serum cap was charged with 0.50 g (1.45 mmol, 2.8×) of $(\mu\text{-}S_2)Fe_2(CO)_6$ and flushed with nitrogen. Benzene (30 mL) was added, and the resulting solution was cannulated into the $(PPh_3)_3PdCO$ solution. The reaction mixture immediately turned brown-red and remained that color while it was stirred for 2.5 h. Solvent was removed on a rotary evaporator, leaving a black solid which was extracted with pentane. These washings were combined, concentrated, and chromatographed (silicic acid–pentane) to give a trace amount of $(\mu\text{-}S_2)Fe_2(CO)_6$. The remaining solid was dissolved in 40% CH_2Cl_2/pentane and applied to the column. Elution with 40% CH_2Cl_2/pentane yielded a brown-red band which, upon removal of solvent, gave 0.479 g (0.492 mmol, 94% yield) of $[\mu\text{-}(Ph_3P)_2PdS_2]Fe_2(CO)_6$ as an air-stable, purple-brown, crystalline solid. After recrystallization from a CH_2Cl_2/pentane mixture (mp 160 °C dec), it was identified by comparison of its IR and NMR spectra to those of an authentic sample (prepared earlier by $(\mu\text{-}S_2)Fe_2(CO)_6/LiEt_3BH/(Ph_3P)_2PdCl_2$ method.[1b])

Reaction between (μ-Dithio)bis(tricarbonyliron) and [Bis(1,2-diphenylphosphino)ethane]nickel Dicarbonyl. A 100-mL Schlenk flask equipped with a serum cap and a stir-bar was charged with 0.688 g (2 mmol) of $(\mu\text{-}S_2)Fe_2(CO)_6$ and 1.03 g (2 mmol) of $(diphos)Ni(CO)_2$ (Strem). Benzene (40 mL) was added by syringe, and the resulting solution was stirred for 24 h at room temperature. Solvent was removed from the red-brown solution on a rotary evaporator, leaving a brown-black solid which was chromatographed on silicic acid. Pentane eluted a trace of $(\mu\text{-}S_2)Fe_2(CO)_6$. Dichloromethane eluted a red-brown band which, upon removal of solvent, gave 1.24 g (1.55 mmol, 77% yield) of $[\mu\text{-}(diphos)NiS_2]Fe_2(CO)_6$ as a brown-black air-stable solid, which was recrystallized from CH_2Cl_2: mp 160–162 °C. IR (CH_2Cl_2): 1480 w, 1429 w, 1101 m, 875 w, 611 m cm^{-1}. Terminal carbonyl region: 2048 s, 2007 vs, 1970 s, 1960 sh cm^{-1}. ^1H NMR (CD_2Cl_2): δ 2.20 (d, $^2J(P-H)$ = 17 Hz, 1 H, $-PCH_2CH_2P-$), 7.34–7.98 (m, 5 H, $-PPh$). Anal. Calcd for $C_{32}H_{24}Fe_2O_6NiP_2S_2$: C, 47.98; H, 3.02. Found: C, 48.10; H, 3.30.

Reaction between (μ-Dithio)bis(tricarbonyliron) and Bis(cyclopentadienyl)titanium Dicarbonyl. A 200-mL flask equipped with a magnetic stir-bar and a serum cap was charged with 1.013 g (4.33 mmol) of $Cp_2Ti(CO)_2$. Benzene (25 mL) was added to give a deep red solution. A 100-mL flask fitted with a serum cap was charged with 2.064 g (6 mmol) of $(\mu\text{-}S_2)Fe_2(CO)_6$ and flushed with nitrogen. After 50 mL of THF was added, the solution was cannulated into the $Cp_2Ti(CO)_2$ solution. The resulting reaction solution was stirred for 18 h, after which time the dark red solution contained a black precipitate. Solvent was removed on a rotary evaporator, leaving a black solid which was extracted with pentane. These washings were combined, concentrated, and chromatographed (silicic acid–pentane) to give 0.890 g (2.59 mmol) of $(\mu\text{-}S_2)Fe_2(CO)_6$. Subsequently, the black solid was washed with dichloromethane and acetone until the washings were colorless. This left 1.422 g (2.72 mmol, 63% yield based on $Cp_2Ti(CO)_2$) of $(\eta^5\text{-}C_5H_5)_2TiS_2Fe_2(CO)_6$ as an air-stable, black solid which was insoluble in pentane, CH_2Cl_2, MeOH, acetone, THF, and DMSO: mp >360 °C. IR (KBr pellet): 790 m, 595 m, 570 m, 550 m cm^{-1}. Terminal carbonyl region: 2036 s, 2016 s, 1973 vs, 1965 vs, 1943 vs cm^{-1}. Anal. Calcd for $C_{16}H_{10}Fe_2O_6S_2Ti$: C, 36.82; H, 1.93. Found: C, 37.02; H, 1.98.

Reaction between (μ-Dithio)bis(tricarbonyliron) and 2 Equiv of Dicobalt Octacarbonyl. A 200-mL round-bottomed flask equipped with a stir-bar, a serum cap, and a nitrogen inlet needle was charged with 1.00 g (2.91 mmol) of $(\mu\text{-}S_2)Fe_2(CO)_6$ and 2.00 g (5.82 mmol, 2×) of $Co_2(CO)_8$ (Strem) and then was flushed with nitrogen. After THF (50 mL) was added, the flask was wrapped in aluminum foil and the reaction solution then was stirred for 19 h. Solvent was removed from the resulting black solution on a rotary evaporator, leaving a black solid which was applied (in pentane) to a silicic acid filtration chromatography column. Dichloromethane eluted a black band which upon removal of solvent gave 2.622 g (5.72 mmol, 98% yield) of (μ_3-thio)iron–dicobalt nonacarbonyl, $SFeCo_2(CO)_9$, as air-stable, black crystals. Recrystallization from pentane [mp 110 °C dec (lit.[4] mp 112 °C/dec)] gave pure material. IR (CH_2Cl_2): terminal carbonyl region, 2106 m, 2067 vs, 2054 vs, 2041 s, 2029 m, 1973 m cm^{-1}. Mass spectrum: molecular ion at m/e 458 with fragment ions corresponding to $M - (CO)_x$ for x = 1–9. Anal. Calcd for $C_9Co_2FeO_9S_2$: C, 23.61; H, 0.00. Found: C, 23.43; H, 0.07.

Reaction between (μ-Dithio)bis(tricarbonyliron) and Diiron Nonacarbonyl. A 200-mL round-bottomed flask equipped with a stir-bar, a serum cap, and a nitrogen inlet needle was charged with 1.00 g (2.91 mmol) of $(\mu\text{-}S_2)Fe_2(CO)_6$ and 1.82 g (5.00 mmol) of $Fe_2(CO)_9$ (Strem) and then was flushed with nitrogen. After THF (50 mL) was added, the flask was wrapped in aluminum foil and the reaction solution was stirred for 16.5 h at room temperature. Solvent was removed from the resulting purple solution on a rotary evaporator, leaving a purple-black solid which was chromatographed (silicic acid–pentane). Elution with 20% CH_2Cl_2/pentane yielded a purple band which, upon removal of solvent, gave 1.405 g (2.90 mmol, 100% yield) of $S_2Fe_3(CO)_9$ as air-stable, purple crystals, which were recrystallized from pentane: mp 111–113 °C (lit.[54] 114 °C). IR (pentane): terminal carbonyl region, 2065 vs, 2042 vs, 2026 s, 2010 sh, 1986 w cm^{-1}. Mass spectrum: molecular ion at m/e 484 with fragment ions corresponding to $M - (CO)_x$ for x = 1–9.

Reaction between (μ-Dithio)bis(tricarbonyliron) and (Cyclopentadienyl)cobalt Dicarbonyl. A 200-mL round-bottomed flask equipped with a magnetic stir-bar and a serum stopper was charged with 0.50 g (1.45 mmol) of $(\mu\text{-}S_2)Fe_2(CO)_6$ and then flushed with nitrogen. THF (50 mL) and 0.705 g (4.06 mmol, 2.7×) of $(\eta^5\text{-}C_5H_5)Co(CO)_2$ were added by syringe, and the resulting solution was stirred for 20 h in the dark. (The flask was covered with aluminum foil.) Solvent was removed under reduced pressure, and the residue was chromatographed (silicic acid). Pentane eluted a red band which gave 0.302 g of an oily red solid. (It was shown by its IR spectrum to be a mixture of $(\mu\text{-}S_2)Fe_2(CO)_6$ and $CpCo(CO)_2$.) Subsequent elution with 4:1 pentane/dichloromethane gave a dark purple band which, upon removal of solvent, gave 0.439 g (0.94 mmol) of $(\mu\text{-}CpCoS_2)Fe_2(CO)_6$ as a black, air-stable, crystalline solid in 68% yield. Recrystallization from pentane gave material with a melting point of 122 °C dec. ^1H NMR ($CDCl_3$, 60 MHz): δ 5.85 (s, C_5H_5). ^{13}C NMR ($CDCl_3$): δ_C

---

[54] Nametkin, N. S.; Tyurin, V. D.; Kukina, M. A. *J. Organomet. Chem.* **1978**, *149*, 355.

84.35 (s, Cp), 205.89 (s, CO). IR (CH_2Cl_2): 1415 w, 1010 w, 840 m, 590 m, 560 m cm^{-1}. Terminal carbonyl region: 2068 s, 2042 vs, 1993 vs cm^{-1}. Mass spectrum: *m/z* (relative intensity) 468 (0.1, M^+), 440 (0.5, $M^+ - CO$), 412 (0.5, $M^+ - 2CO$), 386 (0.5, $M^+ - 3CO$), 356 (0.6, $M^+ - 4CO$), 328 (2.3, $M^+ - 5CO$), 300 (19.6, $M^+ - 6CO$), 235 (48.3, $CoS_2Fe_2^+$), 176 (48.0, $S_2Fe_2^+$), 144 (19.6, SFe_2^+), 124 (74.5, CpCo), 59 (56.7, Co), 56 (100.0, Fe^+). Anal. Calcd for $C_{11}H_5COFe_2O_6S_2$: C, 28.24; H, 1.08. Found: C, 28.34; H, 1.17.

Reaction between (μ-Dithio)bis(tricarbonyliron) and (Pentamethylcyclopentadienyl)cobalt Dicarbonyl. A 100-mL Schlenk flask equipped with a serum stopper and a magnetic stir-bar was charged with 0.743 g (2.97 mmol) of $(\eta^5\text{-}Me_5C_5)Co(CO)_2$. The flask was removed from the drybox and flushed with nitrogen. Benzene (50 mL) was added by syringe, and the resulting red solution was stirred and cooled to ~5 °C. Against a counterflow of nitrogen 1.00 g (2.91 mmol) of $(\mu\text{-}S_2)Fe_2(CO)_6$ was added to the stirred solution. The reaction mixture was allowed to warm to room temperature and was stirred for 16 h. Solvent was removed under reduced pressure, and the black residue was purified by chromatography on silicic acid. A trace of $(\mu\text{-}S_2)Fe_2(CO)_6$ was eluted with 9:1 petroleum ether/dichloromethane. Subsequently a dark purple band was eluted with 3:1 petroleum ether/dichloromethane which, upon removal of solvent, gave 1.558 g (2.90 mmol) of $(\mu\text{-}Me_5C_5CoS_2)Fe_2(CO)_6$ as a black air-stable, crystalline solid in 99% yield. Recrystallization from 3:1 petroleum ether/dichloromethane gave pure material, mp 154–160 °C. ^1H NMR (CD_2Cl_2, 90 MHz): δ 2.18 (s, CH_3). ^{13}C NMR (CD_2Cl_2, 67.9 MHz): δ_C 11.33 (q, *J* = 128.4 Hz, CH_3), 99.07 (s, Me_5C_5), 206.33 (s, C$\equiv$O). IR (CH_2Cl_2): terminal carbonyl region, 2057 s, 2015 vs, 1987 sh, 1978 s cm^{-1}. Mass spectrum (FD, 12 mA, CH_2Cl_2): *m/z* (relative intensity, calcd intensity) 536 (15, 12.9), 537 (0, 2.4), 538 (100, 100), 539 (35, 20.4), 540 (25, 10). Anal. Calcd for $C_{16}H_{15}CoFe_2O_6S_2$: C, 35.72; H, 2.81. Found: C, 35.67; H, 2.89.

Reaction between (μ-Dithio)bis(tricarbonyliron) and (Pentamethylcyclopentadienyl)cobalt Carbonyl Dimer. A 250-mL Schlenk flask equipped with a magnetic stir-bar and a serum stopper was charged with 0.490 g (1.15 mmol) of $[(\eta^5\text{-}Me_5C_5)Co(\mu\text{-}CO)]_2$. Toluene (35 mL) was added, and an emerald green solution was obtained. The flask was removed from the drybox and flushed with nitrogen. The solution was cooled to 0 °C in an ice bath. At the same time, a 100-mL Schlenk flask equipped with a serum stopper was charged with 0.189 g (0.55 mmol) of $(\mu\text{-}S_2)Fe_2(CO)_6$ and flushed with nitrogen. Toluene (30 mL) was added by syringe, and the resulting red solution was cooled to 0 °C. It was added dropwise to the green solution through a 20 gauge cannula. After the solution, was stirred for 1 h at 0 °C, thin-layer chromatography (TLC) showed that $(\mu\text{-}S_2)Fe_2(CO)_6$ had completely disappeared and that no $(\mu\text{-}S)_2Fe_3(CO)_9$ had been formed. Also, a purple spot that did not elute, corresponding to the cobalt starting material, was observed, along with a brown spot that moved in 4:1 pentane/dichloromethane. Therefore, an additional 0.189 g (1.10 mmol, total) of $(\mu\text{-}S_2)Fe_2(CO)_6$ in toluene (30 mL) was added in the same manner as before and the solution was stirred for 1 h at 0 °C. Solvent was removed under reduced pressure at 0 °C, and a dark residue was obtained. The solid was purified by column chromatography under nitrogen on Florisil. Petroleum ether eluted a trace of the cobalt starting material. Subsequent elution with 4:1 petroleum ether/dichloromethane gave a brown band which, upon removal of solvent, gave 0.761 g (1.03 mmol) of a black, air-sensitive, crystalline solid in 94% yield. The compound was recrystallized from dichloromethane/diethyl ether, mp 154–160 °C dec and formulated as **16**, on the basis of its analysis and spectroscopic properties. ^1H NMR (CD_2Cl_2, 250 MHz): δ 1.59 (s, CH_3). ^{13}C NMR (CD_2Cl_2, 67.9 MHz): δ_C 8.48 (q, *J* = 128.3 Hz, CH_3), 102.86 (d, Me_5C_5), 209.46 (s, C$\equiv$O), 250.83 (s, μ-CO). IR (CH_2Cl_2): 2952 vw, 1380 m, 1359 vw, 1260 vw, 1160 vw, 1018 w, 690 b, 592 b cm^{-1}. Terminal carbonyl region: 2049 s, 2008 vs, 1980 s cm^{-1}. Bridging carbonyl region: 1809 s cm^{-1}. Mass spectrum (FD, 10 mA, CH_2Cl_2): *m/z* (relative intensity, calcd intensity) 786 (22, 12.9), 787 (13, 3.9), 788 (100, 100), 789 (35, 32.5), 790 (22, 13.4), 791 (11, 3.2), M^+; 732 (84), $M^+ - 2CO$. Anal. Calcd for $C_{28}H_{30}Co_2Fe_2O_8S_2$: C, 42.37; H, 3.84. Found: C, 42.01; H, 3.83.

Reaction between (μ-Dithio)bis(tricarbonyliron) and μ-[$(Me_5C_5)Co(\mu\text{-}CO)]_2$ $(\mu_3\text{-}S)_2Fe_2(CO)_6$. A 50-mL round-bottomed flask equipped with a magnetic stir-bar and a serum stopper was charged with 0.065 g (0.088 mmol) of $\mu\text{-}[(\eta^5\text{-}Me_5C_5)Co(\mu\text{-}CO)]_2(\mu_3\text{-}S)_2Fe_2(CO)_6$ and 0.080 g (0.232 mmol) of $(\mu\text{-}S_2)Fe_2(CO)_6$ in the drybox. Benzene (20 mL) was added, the solution was stirred, and the reaction was followed by TLC. After 2 weeks all of the cobalt-containing starting material had disappeared. Solvent was removed under reduced pressure, and the flask was removed from the drybox. The black residue was purified by column chromatography (silicic acid). Petroleum ether eluted a red band which, upon removal of solvent, gave 0.048 g (0.14 mmol, 60%) of $(\mu\text{-}S_2)Fe_2(CO)_6$. Subsequent elution with 9:1 petroleum ether/dichloromethane gave a dark purple band. Removal of the solvent gave 0.094 g (0.175 mmol) of $(\mu\text{-}Me_5C_5CoS_2)Fe_2(CO)_6$ as a black, air-stable, crystalline solid in 99% yield. The complex was recrystallized from dichloromethane/petroleum ether, mp 155–160 °C dec, and identified by comparison with an authentic sample prepared as described above.

X-ray Data Collection. Black-purple crystals of $(\eta^5\text{-}C_5Me_5)Co(\mu_3\text{-}S)_2Fe_2(CO)_6$ and $[(\eta^5\text{-}C_5Me_5)Co(\mu\text{-}CO)]_2(\mu\text{-}S)_2Fe_2(CO)_6$ were mounted in air on glass fibers. Unit cell dimensions for both were obtained from least-squares analyses of the setting angles of 25 reflections which were accurately centered at 22 °C on an Enraf-Nonius CAD4 diffractometer using Mo Kα radiation. In the former the *mmm* diffraction symmetry and the systematic absences ($h00$, $h = 2n + 1$; $0k0$, $k = 2n + 1$; $00l$: $l = 2n + 1$) were consistent with the orthorhombic space group $P2_12_12_1$ whereas in the latter the $2/m$ diffraction symmetry and the absences ($0k0$, $k = 2n + 1$) were consistent with the monoclinic space groups $P2_1$ and $P2_1/m$. The centrosymmetric space group $P2_1/m$ was ultimately confirmed as correct based on the successful refinement of the structure in this space group and the location of all hydrogen atoms, the positions of which were consistent with the crystallographically imposed mirror symmetry in the molecule.

Intensity data were collected on the CAD4 diffractometer in the bisecting mode employing the ω–2θ scan technique and using Mo Kα radiation. Backgrounds were scanned for 25% of the peak widths on each end of the scans. Three reflections were monitored periodically for each structure as a check for crystal decomposition or movement. No significant variation in these standards was observed so no correction was applied. An ignorance factor of 0.04 was used in processing each data set.[55] Table VII should be consulted for details about the crystals and data collection.

Structure Solution and Refinement. Both structures were solved by using MULTAN[56] to locate the Co, Fe, and S atoms. All other atoms were located in subsequent differences Fourier maps. Full-matrix, least-squares techniques were used for the refinements,[57] utilizing the usual neutral atom scattering factors[58] and anomalous dispersion terms.[59] All non-hydrogen atoms were refined anisotropically. Hydrogen atoms were located but were input in their idealized positions, which were derived from the observed ones by assuming idealized sp^3 geometries of the attached carbons and C–H distances of 0.95 Å. The hydrogen positions were allowed to ride on the attached carbons with the positional changes calculated for the latter being applied to the hydrogen positions. Hydrogen atoms were assigned isotropic thermal parameters of 1.0 Å^2 greater than the equivalent isotropic *B* of the attached carbon atom. Absorption corrections were applied to the data using the method of Walker and Stuart.[60]

Comparisons of the observed and calculated structure amplitudes showed no unusual features for either structure. In the final difference Fourier maps the highest 10 residuals (which were below 0.5 (1) and 0.49 (7) e Å^{-3} for the trinuclear and tetranuclear species, respectively) were in the vicinities of the methyl groups and the metals. Positional parameters and equivalent isotropic

---

(55) Doedens, R. J.; Ibers, J. A. *Inorg. Chem.* **1967**, *6*, 204.

(56) Germain, G.; Main, P.; Woolfson, M. M. *Acta Crystallogr., Sect. A: Cryst. Phys., Diffr., Theor. Gen. Crystallogr.* **1971**, *A27*, 368.

(57) Programs used were those of the Enraf-Nonius Structure Determination Package by B. A. Frenz, in addition to some local programs by R. G. Ball.

(58) (a) Stewart, R. F.; Davidson, E. F.; Simpson, W. T. *J. Chem. Phys.* **1965**, *42*, 3175. (b) Cromer, D. T.; Waber, J. F. *International Tables for X-ray Crystallography*; Kynoch: Birmingham, England, 1974; Vol. IV, Table 2.2A.

(59) Cromer, D. T.; Liberman, D. *J. Chem. Phys.* **1970**, *53*, 1891.

(60) Walker, N.; Stuart, D. *Acta Crystallogr., Sect. A: Found. Crystallogr.* **1983**, *A39*, 1581.

Table VII. Summary of Crystal Data and Details of Intensity Collection for $(\eta^5\text{-}C_5Me_5)Co(\mu_3\text{-}S)_2Fe_2(CO)_6$ and $[(\eta^5\text{-}C_5Me_5)Co(\mu\text{-}CO)]_2(\mu\text{-}S)_2Fe_2(CO)_6$

	$(\eta^5\text{-}C_5Me_5)Co(\mu_3\text{-}S)_2Fe_2(CO)_6$	$[(\eta^5\text{-}C_5Me_5Co(\mu\text{-}CO)]_2(\mu\text{-}S)_2Fe_2(CO)_6$
fw	538.05	788.23
space group	$P2_12_12_1$ (No. 19)	$P2_1/m$ (No. 11)
a, Å	8.848 (5)	10.712 (1)
b, Å	12.571 (3)	14.837 (2)
c, Å	18.707 (3)	10.8215 (9)
β, deg		115.537 (8)
V, $Å^3$	2080.6	1551.8
ρ(calcd), g cm^{-3}	1.718 (*Z* = 4)	1.687 (*Z* = 2)
radiatn	Mo K*α*, λ = 0.71073 Å, graphite monochromated	Mo K*α*, graphite monochromated
temp, °C	22	22
detector aperature, mm	4.0(2.00 + 1.00 tan *θ*)	4.0(2.00 + 1.00 tan *θ*)
takeoff angle, deg	3.0	3.0
2*θ* limit, deg	60.0	54.0
scan type	*ω*/2*θ*	*ω*/2*θ*
scan width	(0.70 + 0.347 tan *θ*) in *ω*	(0.75 + 0.347 tan *θ*) in *ω*
scan speed, deg min^{-1}	variable, between 1.67 and 10.0	variable, between 1.11 and 6.67
indices collected	*h,k,l*	*h,k,±l*
unique data collected	3439	3693
reflections obsd	2031	2409
abs coeff *μ*, cm^{-1}	23.843	21.413
cryst dimers, mm	0.35 × 0.20 × 0.18	0.29 × 0.25 × 0.10
range in abs correctn factors	1.280–0.514	1.427–0.653
final no. of parameters varied	244	202
error in observn of unit weight	1.334	1.357
R	0.058	0.033
R_w	0.051	0.040

Table VIII. Positional Parameters and Equivalent Isotropic *B*'s[a] for the Non-Hydrogen Atoms in $(\eta^5\text{-}C_5Me_5)Co(\mu_3\text{-}S)_2Fe_2(CO)_6$

atom	*x*	*y*	*z*	B_{eq} ($Å^2$)
Co	0.0034 (1)	0.56691 (7)	−0.10772 (5)	2.93 (2)
Fe(1)	−0.1635 (1)	0.40890 (8)	−0.08010 (5)	3.59 (2)
Fe(2)	−0.1643 (1)	0.5788 (1)	−0.21827 (6)	4.03 (2)
S(1)	−0.0335 (2)	0.4370 (2)	−0.1811 (1)	3.85 (4)
S(2)	−0.2409 (2)	0.5745 (2)	−0.1046 (1)	3.54 (4)
O(1)	−0.4070 (8)	0.2740 (5)	−0.1349 (4)	7.0 (2)
O(2)	−0.047 (1)	0.2438 (6)	−0.0386 (4)	11.4 (3)
O(3)	−0.255 (1)	0.4439 (6)	0.0679 (3)	9.0 (2)
O(4)	0.0496 (8)	0.5971 (7)	−0.3369 (3)	8.3 (2)
O(5)	−0.2816 (9)	0.7974 (6)	−0.2287 (5)	10.5 (3)
O(6)	−0.4161 (7)	0.4717 (7)	−0.2896 (4)	8.5 (2)
C(1)	−0.313 (1)	0.3268 (6)	−0.1128 (5)	4.6 (2)
C(2)	−0.034 (1)	0.3074 (7)	−0.0546 (5)	6.7 (3)
C(3)	−0.223 (1)	0.4276 (8)	0.0104 (4)	5.5 (2)
C(4)	−0.0350 (9)	0.5897 (8)	−0.2923 (4)	5.6 (2)
C(5)	−0.232 (1)	0.7140 (8)	−0.2267 (5)	6.5 (2)
C(6)	−0.316 (1)	0.5143 (8)	−0.2630 (5)	5.5 (2)
C(7)	0.1541 (9)	0.5704 (7)	−0.0227 (4)	5.4 (2)
C(8)	0.2309 (8)	0.5633 (7)	−0.0871 (5)	6.6 (2)
C(9)	0.198 (1)	0.6531 (7)	−0.1283 (5)	5.5 (2)
C(10)	0.096 (1)	0.7130 (6)	−0.0881 (5)	6.3 (2)
C(11)	0.0694 (9)	0.6619 (7)	−0.0244 (4)	5.0 (2)
C(12)	0.172 (1)	0.4992 (9)	−0.0431 (6)	15.0 (4)
C(13)	0.339 (1)	0.4718 (9)	−0.1057 (7)	15.0 (5)
C(14)	0.266 (1)	0.683 (1)	−0.1984 (6)	16.2 (4)
C(15)	0.035 (2)	0.8206 (8)	−0.1084 (7)	14.1 (5)
C(16)	−0.025 (1)	0.701 (1)	0.0364 (5)	11.3 (3)

[a] Equivalent isotropic thermal parameter (B_{eq}) defined as $(8\pi^2/3)(U_{11} + U_{22} + U_{33})$.

thermal parameters are given in Tables VIII and IX. Additional information is available as supplementary material.

Calculational Details. The Fenske–Hall calculations[10] were carried out by using geometries obtained from structural studies where these were available. For the Ge studies we assumed an angle HGeH of 109°, a Ge–H bond length of 1.53 Å, and Ge–S bond lengths of 2.16 Å. The Fe–S bond length was maintained at 2.25 Å in the θ = 95° case. Details of the atomic orbitals that were used as a basis set may be found in an earlier study.[61] The basis set for the Ge atom was obtained from a supplement to the work of Clementi.[62]

Table IX. Positional Parameters and Equivalent Isotropic *B*'s[a] for the Non-Hydrogen Atoms in $[(\eta^5\text{-}C_5Me_5)Co(\mu\text{-}CO)]_2(\mu\text{-}S)_2Fe_2(CO)_6$

atom	*x*	*y*	*z*	B_{eq} ($Å^2$)
Co(1)	0.23122 (5)	0.2500	0.24837 (5)	2.25 (1)
Co(2)	0.05726 (5)	0.2500	0.34614 (5)	2.41 (1)
Fe	0.41163 (4)	0.33396 (3)	0.62383 (4)	2.794 (9)
S(1)	0.4223 (1)	0.2500	0.4545 (1)	2.60 (2)
S(2)	0.2188 (1)	0.2500	0.5699 (1)	2.93 (2)
O(1)	0.7112 (3)	0.3588 (2)	0.7301 (3)	5.78 (8)
O(2)	0.4123 (4)	0.3689 (3)	0.8889 (3)	9.0 (1)
O(3)	0.3501 (3)	0.5203 (2)	0.5276 (3)	6.34 (9)
O(4)	0.1425 (2)	0.4248 (2)	0.2942 (2)	3.88 (5)
C(1)	0.5942 (4)	0.3500 (3)	0.6883 (3)	3.81 (8)
C(2)	0.4110 (4)	0.3553 (3)	0.7847 (4)	5.0 (1)
C(3)	0.3674 (4)	0.4460 (3)	0.5586 (4)	4.15 (9)
C(4)	0.1470 (3)	0.3465 (2)	0.2996 (3)	2.63 (6)
C(5)	0.1642 (3)	0.2982 (2)	0.0438 (3)	3.38 (7)
C(6)	0.2991 (3)	0.3276 (3)	0.1248 (3)	3.74 (7)
C(7)	0.3843 (4)	0.2500	0.1714 (4)	4.5 (1)
C(8)	0.0455 (5)	0.3581 (3)	−0.0420 (4)	6.5 (1)
C(9)	0.3459 (5)	0.4242 (3)	0.1483 (4)	7.8 (1)
C(10)	0.5386 (5)	0.2500	0.2424 (5)	9.1 (3)
C(11)	−0.0865 (3)	0.2981 (3)	0.4164 (3)	4.16 (8)
C(12)	−0.1305 (3)	0.3274 (3)	0.2826 (4)	4.48 (9)
C(13)	−0.1547 (4)	0.2500	0.1985 (5)	4.9 (1)
C(14)	−0.0589 (4)	0.3552 (4)	0.5400 (4)	9.0 (1)
C(15)	−0.1604 (5)	0.4226 (3)	0.2337 (7)	10.3 (2)
C(16)	−0.2217 (7)	0.2500	0.0455 (6)	12.0 (4)

[a] $B_{eq} = (8\pi^2/3)(U_{11}/\sin^2\beta + U_{22} + U_{33}/\sin^2\beta + 2U_{13}\cos\beta/\sin^2\beta)$.

Acknowledgment. We are grateful to the National Science Foundation for support of the preparative work at M.I.T., to the University of Alberta and the Natural Sciences and Engineering Research Council of Canada for support of the structural study at the University of Alberta, and to the M.I.T. Mass Spectrometry Facility (supported by N.I.H. Division of Research Resources, Grant No. RR00317, K. Biemann, principal investigator) for mass

---

(61) DeKock, R. L.; Wong, K. S.; Fehlner, T. P. *Inorg. Chem.* **1982**, *21*, 3203.

(62) Clementi, E. *IBM J. Res. Dev.* **1965**, *9*, 2.

spectra. M.C. also thanks NSERC Canada for partial funding of the diffractometer. Acknowledgment is also made to the donors of the Petroleum Research Fund, administered by the American Chemical Society, for support of the work done at Calvin College on the Fenske–Hall calculations.

Registry No. **1**, 14243-23-3; **2**, 22364-22-3; **3a**, 75249-93-3; **3b**, 75249-92-2; **4**, 116888-32-5; **8**, 116888-33-6; **13**, 69657-52-9; **14**, 116888-35-8; $(\eta^5\text{-}\mathrm{C_5H_5})\mathrm{Co(CO)_2}$, 12078-25-0; $(\eta^5\text{-}\mathrm{C_5Me_5})\mathrm{Co(CO)_2}$, 12129-77-0; $\mathrm{(PPh_3)_4Pt}$, 14221-02-4; $\mathrm{(PPh_3)_4Pd}$, 14221-01-3; $\mathrm{(diphos)Ni(CO)_2}$, 15793-01-8; $\mathrm{Cp_2Ti(CO)_2}$, 12129-51-0; $\mathrm{Co_2(CO)_8}$, 10210-68-1; $\mathrm{Fe_2(CO)_9}$, 15321-51-4; $\mathrm{S_2Fe_3(CO)_9}$, 22309-04-2; $(\mu\text{-}\mathrm{Me_5C_5CoS_2})\mathrm{Fe_2(CO)_6}$, 116888-34-7.

Supplementary Material Available: Tables of anisotropic thermal parameters, idealized hydrogen parameters, bond lengths and angles within the carbonyl and Cp* groups, and weighted least-squares planes (9 pages); listings of observed and calculated structure amplitudes (23 pages). Ordering information is given on any current masthead page.

Synthesis and Spectral Characterization of a Series of Iron and Ruthenium Benzylidene Complexes, $\mathrm{Cp(CO)(L)M{=}CH(C_6H_4R)^+}$ (M = Fe, Ru; L = CO, $\mathrm{PPh_3}$; R = *p*-H, *p*-F, *p*-$\mathrm{CH_3}$, *p*-$\mathrm{OCH_3}$). Barriers to Aryl Rotation and Benzylidene Transfer Reactions

M. Brookhart,* William B. Studabaker, and M. Beth Humphrey

Department of Chemistry, The University of North Carolina at Chapel Hill,
Chapel Hill, North Carolina 27599-3290

G. Ronald Husk

U. S. Army Research Office, P.O. Box 12211, Research Triangle Park, North Carolina 27709

Received March 29, 1988

The α-ether complexes $\mathrm{Cp(CO)_2Fe\text{-}CH(OCH_3)C_6H_4R}$ (**7a**, R = H; **7b**, R = *p*-F; **7c**, R = *p*-$\mathrm{CH_3}$; **7d**, R = *p*-$\mathrm{OCH_3}$; **7e**, R = *m*-$\mathrm{OCH_3}$; **7f**, R = *p*-$\mathrm{CF_3}$), $\mathrm{Cp(CO)_2Ru\text{-}CH(OCH_3)C_6H_4R}$ (**10a**, R = H; **10b**, R = *p*-F; **10c**, R = *p*-$\mathrm{CH_3}$; **10d**, R = *p*-$\mathrm{OCH_3}$), and $\mathrm{Cp(CO)(PPh_3)M\text{-}CH(OCH_3)C_6H_4R}$ (**11a–d**, M = Fe; **15a–d**, M = Ru; **a**, R = H; **b**, R = *p*-F; **c**, R = *p*-$\mathrm{CH_3}$; **d**, R = *p*-$\mathrm{OCH_3}$) were synthesized by methylation of the corresponding benzoyl complexes followed by hydride reduction. Treatment of the α-ether complexes with trimethylsilyl triflate gave the series of benzylidene complexes $\mathrm{Cp(CO)_2M{=}CH(C_6H_4R)^+}$ (**1**, M = Fe; **2**, M = Ru) and $\mathrm{Cp(CO)(PPh_3)M{=}CH(C_6H_4R)^+}$ (**3**, M = Fe; **4**, M = Ru) which were characterized by ^{1}H and ^{13}C NMR spectroscopy. Barriers to aryl ring rotation were measured by dynamic ^{1}H NMR methods and found to be 9.4 (**1a**), 10.2 (**1b**), 10.7 (**1c**), 13.5 (**1d**), 10.6 (**2b**), 10.9 (**2c**), 14.5 (**2d**), 9.0 (**3b**), 9.0 (**3c**), 10.9 (**3d**), 9.1 (**4b**), 9.2 (**4c**), and 11.1 (**4d**) kcal/mol. Barriers vary in the expected way with arene substituents and a reasonable Hammett σ^+/ρ correlation exists for 1 (ρ = ca. +5). The nearly identical barriers observed for Fe and Ru analogues suggest similar positive charge densities at $\mathrm{C_\alpha}$ in these analogues. Benzylidene transfers to propene to give 1-aryl-2-methylcyclopropanes were carried out by using **1a–f**. The cis/trans isomer ratios are all ca. 8 except for **1d** where cis/trans = 2. Mechanistic implications of this data are considered.

Electrophilic transition-metal carbene complexes $\mathrm{L_nM{=}CHR}$ (R = H, alkyl, aryl) are much less stable than classical, Fischer-type heteoatom-substituted carbene complexes, especially where the organometallic fragment is not electron-rich. For example, the complexes $\mathrm{Cp(CO)_2Fe{=}CH_2^+}$[1] and $\mathrm{Cp(CO)_2Fe{=}CHCH_3^+}$[2-4] (Cp = $\eta^5\text{-}\mathrm{C_5H_5}$) are implicated as reactive intermediates but have escaped direct observation by usual spectroscopic techniques.[5] Analogues of these highly electrophilic species may be stabilized either by substitution of better donor ligands for the π-acid CO ligands or by substitution of hydrocarbon substituents at the carbene carbon which are effective at delocalizing positive charge. Hence, the phosphine-substituted derivatives $\mathrm{Cp(Ph_2PCH_2CH_2PPh_2)Fe{=}CH_2^+}$[6] and $\mathrm{Cp(CO)(PPh_3)Fe{=}CHCH_3^+}$[2] have been characterized spectroscopically at low temperatures and aryl-, vinyl-, and cyclopropyl-substituted complexes $\mathrm{(CO)_5W{=}CHPh}$,[7] $\mathrm{Cp(CO)_2Fe{=}CHPh^+}$,[8] $\mathrm{Cp(CO)_2Fe{=}CHCH{=}C(CH_3)_2^+}$,[9,10] and $\mathrm{Cp(CO)_2Fe{=}CH\text{-}}c\text{-}\mathrm{C_3H_5^+}$[11] have been described. These complexes are sufficiently

---

(1) (a) Jolly, P. W.; Pettit, R. *J. Am. Chem. Soc.* **1965**, *88*, 5044. (b) Riley, P. E.; Capshew, C. E.; Pettit, R.; Davis, R. E. *Inorg. Chem.* **1978**, *17*, 408.

(2) (a) Brookhart, M.; Tucker, J. R.; Husk, G. R. *J. Am. Chem. Soc.* **1981**, *103*, 979. (b) Brookhart, M.; Tucker, J. R.; Husk, G. R. *Ibid.* **1983**, *105*, 258.

(3) (a) Kremer, K. A. M.; Helquist, P.; Kerber, R. C. *J. Am. Chem. Soc.* **1981**, *103*, 1862. (b) Kremer, K. A. M.; Helquist, P. *J. Organomet. Chem.* **1985**, *285*, 231.

(4) Bodnar, T.; Cutler, A. R. *J. Organomet. Chem.* **1981**, *213*, C31.

(5) $\mathrm{Cp(CO)_2Fe{=}CH_2^+}$ has been observed in the gas phase: Stevens, A. E.; Beauchamp, J. L. *J. Am. Chem. Soc.* **1978**, *100*, 2584.

(6) Brookhart, M.; Tucker, J. R.; Flood, T. C.; Jensen, J. *J. Am. Chem. Soc.* **1980**, *102*, 1203.

(7) (a) Casey, C. P.; Polichnowski, S. W. *J. Am. Chem. Soc.* **1977**, *99*, 6097. (b) Casey, C. P.; Polichnowski, S. W. *Ibid.* **1979**, *101*, 7282.

(8) (a) Brookhart, M.; Nelson, G. O. *J. Am. Chem. Soc.* **1977**, *99*, 6099. (b) Brookhart, M.; Humphrey, M. B.; Kratzer, H. J.; Husk, G. R. *Ibid.* **1980**, *102*, 7802. (c) Brookhart, M.; Tucker, J. R.; Husk, G. R. *J. Organomet. Chem.* **1980**, *193*, C23.

(9) (a) Casey, C. P.; Miles, W. H. *Organometallics* **1984**, *3*, 808. (b) Casey, C. P.; Miles, W. H.; Tukada, H. *Ibid.* **1985**, *4*, 2924.

(10) Kuo, G.-H.; Helquist, P.; Kerber, R. C. *Organometallics* **1984**, *3*, 806.

(11) (a) Brookhart, M.; Studabaker, W. B.; Husk, G. R. *Organometallics* **1985**, *4*, 943. (b) Brookhart, M.; Studabaker, W. B.; Husk, G. R. *Ibid.* **1987**, *6*, 1141.

0276-7333/89/2308-0132$01.50/0